arXiv:2509.20067v2 [cs.AI] 25 Sep 2025

MACD: Multi-Agent Clinical Diagnosis with Self-Learned Knowledge for LLM

Wenliang Li[1,2†], **Rui Yan**[1,2†], **Xu Zhang**[1,2†], **Li Chen**[3], **Hongji Zhu**[3], **Jing Zhao**[3], **Junjun Li**[3], **Mengru Li**[3], **Wei Cao**[3], **Zihang Jiang**[1,2], **Wei Wei**[3,*], **Kun Zhang**[1,2,*], and **Shaohua Kevin Zhou**[1,2,4,5,*]

[1]School of Biomedical Engineering, Division of Life Sciences and Medicine, University of Science and Technology of China (USTC), Hefei Anhui, 230026, China

[2]Center for Medical Imaging, Robotics, Analytic Computing & Learning (MIRACLE), Suzhou Institute for Advanced Research, USTC, Suzhou Jiangsu, 215123, China

[3]Department of Radiology, The First Affiliated Hospital of USTC, Division of Life Sciences and Medicine, University of Science and Technology of China, Hefei Anhui, 230001, China

[4]Jiangsu Provincial Key Laboratory of Multimodal Digital Twin Technology, Suzhou Jiangsu, 215123, China

[5]State Key Laboratory of Precision and Intelligent Chemistry, USTC, Hefei Anhui, 230026, China

[†]Equal contribution

[*]Corresponding authors

Abstract

Large language models (LLMs) have demonstrated notable potential in medical applications, yet they face substantial challenges in handling complex real-world clinical diagnoses using conventional prompting methods. Current prompt engineering and multi-agent approaches typically optimize isolated inferences, neglecting the accumulation of reusable clinical experience. To address this, this study proposes a novel Multi-Agent Clinical Diagnosis (MACD) framework, which allows LLMs to self-learn clinical knowledge via a multi-agent pipeline that summarizes, refines, and applies diagnostic insights. It mirrors how physicians develop expertise through experience, enabling more focused and accurate diagnosis on key disease-specific cues. We further extend it to a MACD-human collaborative workflow, where multiple LLM-based diagnostician agents engage in iterative consultations, supported by an evaluator agent and human oversight for cases where agreement is not reached. Evaluated on 4,390 real-world patient cases across seven diseases using diverse open-source LLMs (Llama-3.1 8B/70B, DeepSeek-R1-Distill-Llama 70B), MACD significantly improves primary diagnostic accuracy, outperforming established clinical guidelines with gains up to 22.3% (MACD). In direct comparison with physician-only diagnosis under the same evaluation protocol, MACD achieves comparable or superior performance, with improvements up to 16%. Furthermore, the MACD-human workflow yields an 18.6% improvement over physician-only diagnosis, demonstrating the synergistic potential of human-AI collaboration. Notably, the self-learned clinical knowledge exhibits strong cross-model stability, transferability across LLMs, and capacity for model-specific personalization. The system also generates traceable diagnostic rationales, enhancing transparency and explainability. This work thus presents a scalable self-learning paradigm that bridges the gap between the intrinsic knowledge of LLMs and the demands of real-world clinical practice, advancing towards a reliable, interpretable, and deployable AI-assisted diagnosis.

Introduction

Rapid advancement in Large Language Model (LLM) technology has garnered widespread attention and achieved remarkable success in various natural language processing tasks [1, 2, 3]. In the medical domain, while LLMs achieve human-comparable performance on established medical question-answering benchmarks [4, 5, 6], these tasks use simplified scenarios that do not capture the complexity of open-ended diagnosis [7, 8, 9]. Consequently, a significant performance gap emerges when LLMs confront clinical data from real-world patients [10, 11].

To bridge this gap, prompt engineering offers a flexible and cost-effective approach for guiding a model's reasoning in diagnosis [12, 13, 14], as it does not require large-scale pretraining or parameter updates. Current approaches employ conventional prompting strategies, such as chain-of-thought and few-shot, to enhance diagnostic capabilities by guiding the reasoning of LLMs [15, 16, 17, 18]. However, these methods perform each diagnostic inference independently, paying less attention to the accumulation of reusable experience from clinical practice. In real-world medical settings, physicians rely fundamentally on this accumulated experience to guide their diagnoses. Clinicians efficiently diagnose by applying the knowledge formalized in clinical guidelines and cognitive patterns to enhance diagnostic efficiency and mitigate clinical risks [19, 20]. Inspired by this human-centric model of expertise, integrating the ability to build upon and reuse past diagnostic knowledge is therefore a critical next step for clinical AI systems to mature.

Here, we propose a novel LLM-based multi-agent clinical diagnosis (MACD) framework, which enhances diagnosis accuracy via the systematic accumulation of reusable clinical experience. As illustrated in Fig. 1a, the core idea is to emulate the professional development of a physician by enabling the LLM to autonomously acquire, distill, and internalize clinical knowledge from real-world diagnostic cases over time. Within the framework, as shown in Fig. 1b, there is an ensemble of specialized agents performing distinct cognitive roles: a *knowledge summarizer agent* identifies and extracts salient diagnostic insights from historical cases; a *knowledge refiner agent* consolidates and integrates these insights into structured, evolving self-learned knowledge; and a *diagnostician agent* leverages this curated Self-Learned Knowledge as a critical part of LLM prompt to inform and improve diagnostic reasoning based on LLM. This architecture not only mirrors the experiential learning trajectory of a medical expert but also establishes a scalable, self-improving paradigm for LLM-assisted diagnosis. That is, *Self-Learned Knowledge* enables the diagnostician agent to focus on disease-specific features, bridging the gap between the model's intrinsic knowledge and actual clinical practice. Based on the above MACD framework, this study further develops an MACD-human collaboration workflow. As depicted in Fig. 1c, the workflow integrates diagnostician agents based on diverse LLMs. These diagnostician agents, all leveraging the core self-learning mechanism, engage in multiple rounds of consultation to exchange opinions and reach consensus before producing a final diagnosis. The system also includes an *evaluator agent* responsible for verifying the consistency of the diagnosis.For a small fraction of cases where the

diagnostician agents fail to reach agreement, the workflow introduces human physicians to enable human-LLM collaboration: the outputs of the diagnostician agents serve as decision support, while the final judgment is made by the human physician. In performance evaluations, the collaborative framework significantly outperforms any single agent, validating its scalability and clinical potential.

This study systematically evaluates the effectiveness and generality of the framework, as well as the impact of the base model on its performance. The key findings of the study are as follows: (1) The Self-Learned Knowledge generated by the MACD framework has more practical application value than the Professional Guideline [21, 22, 23, 24, 25, 26, 27, 28, 29] and Mayo Clinic Guideline [30, 31, 32, 33, 34, 35, 36] in clinical diagnosis. The MACD framework achieves more significant performance enhancements, with an up to 22.3% improvement in diagnostic accuracy. When equipped with the Self-Learned Knowledge, the diagnostician agents achieve an accuracy level that approaches or even surpasses that of human physicians, with performance improvements of up to 16% over physicians' diagnoses, showcasing the clinical translational potential of our method. (2) Compared to guideline knowledge, the Self-Learned Knowledge demonstrates superior stability, yielding predictable performance improvements that align with models' intrinsic capabilities (stronger agents obtain higher accuracy, weaker ones lower), and greater transferability, achieving substantial and consistent accuracy gains across diverse LLMs. (3) Self-learned knowledge generated by the MACD framework exhibits model-specific preferences and individualized characteristics, primarily manifested in the fact that each model achieves the highest diagnostic accuracy when using knowledge it has generated itself, compared to knowledge derived from other models. (4) The Self-Learned Knowledge is further evaluated to be effective in the MACD-human collaboration workflow, achieving a notable improvement. The workflow, through its consultation process, provides human physicians with expanded diagnostic perspectives. The Self-Learned Knowledge achieves the highest initial diagnostic consensus rate (58.6%) and the highest effective opinion rate (88.5%) compared to the other two guidelines, indicating its greater capacity to provide physicians with effective diagnostic perspectives. In the subset evaluation where human physicians participate in the consultation process, the self-learned knowledge still achieves the highest diagnostic accuracy of 83.6%, outperforming other guidelines and exceeding the physicians-only diagnosis accuracy by 18.6%. (5) The framework enhances explainability by generating a transparent text-based rationale that links the diagnosis to the case and knowledge, ensuring traceable and interpretable reasoning. In summary, this work not only offers a solution to the problem of LLMs' performance deficits in clinical diagnostic tasks, but also provides a pathway toward building more effective, intelligent, and trustworthy LLM-based open-ended diagnoses in the future.

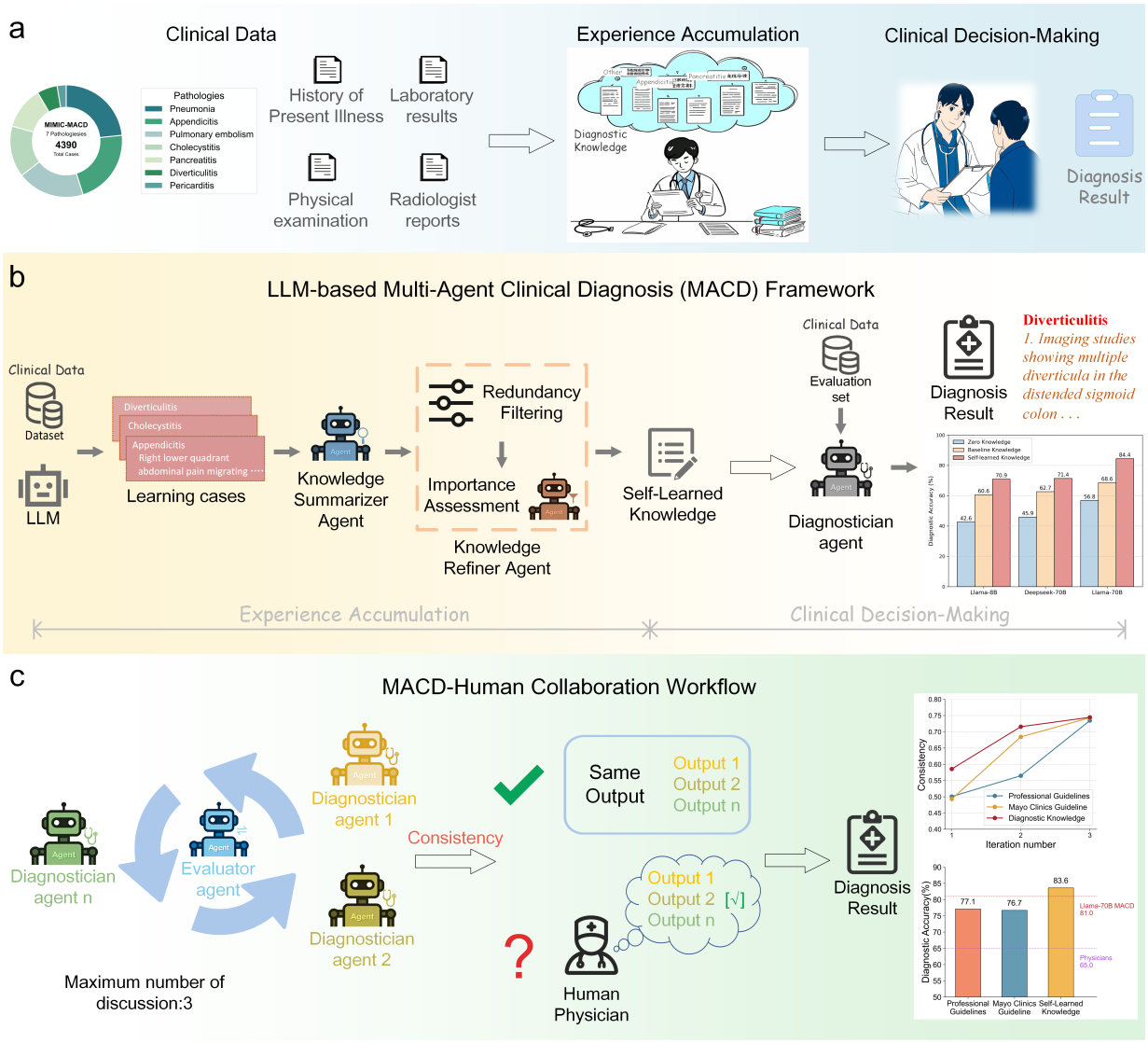

Figure 1: **Overview of the MACD framework.** (a) The core idea of MACD is to emulate the professional development of a physician by enabling the LLM to autonomously acquire, distill, and internalize clinical knowledge from real-world diagnostic cases over time. (b) MACD is formed with a knowledge summarizer agent that identifies and extracts salient diagnostic insights from historical cases, a knowledge refiner agent that consolidates and integrates these insights into a structured, evolving knowledge memory, and a diagnostician agent that leverages this curated experience to inform and improve diagnostic reasoning. (c) A workflow comprising multiple MACD diagnostician agents based on diverse LLMs, called the MACD-human collaboration workflow. The three diagnostic agents jointly discuss the cases. The final output is provided either when agreement is reached or, if the maximum number of discussion is reached without consensus, the final diagnosis is made by human physicians.

Results

Self-Learned Knowledge Superiorly Enhances LLM Clinical Diagnostics

The core idea is to simulate the professional growth of a physician by accumulating expertise from real-world clinical diagnoses. Inspired by how human experts gain experience through continuously summarizing clinical cases, refining diagnostic guidelines in their minds, and applying them, a multi-agent clinical diagnosis (MACD) framework is developed to simulate this cognitive learning process. The MACD framework is operationalized by a team of three collaborating agents: a knowledge summarizer agent that identifies and extracts salient diagnostic insights from historical cases, a knowledge refiner agent that consolidates and integrates these insights into a structured, evolving knowledge memory, and a diagnostician agent that leverages this curated experience to inform and improve diagnostic reasoning. For a detailed description, please refer to the 'Multi-Agent Clinical Diagnosis Framework' section in Methods.

Specifically, the MACD framework uses three different base LLMs with diverse parameter scales and training strategies: the Llama-3.1 models (Llama-3.1-8B-Instruct and Llama-3.1-70B-Instruct) [37] and DeepSeek-R1-Distill-Llama3.3-70B (DeepSeek-70B) [38]. To evaluate the practical efficacy of the Self-Learned Knowledge autonomously generated by the collaboration of the MACD framework, a performance comparison against two authoritative sources of knowledge from the clinical guidelines from professional institutions (Professional Guideline) [21, 22, 23, 24, 25, 26, 27, 28, 29] and diagnostic information from the Mayo Clinic Guideline (Mayo Clinic Guideline) [30, 31, 32, 33, 34, 35, 36] is performed in this study. These guidelines are sourced from the official website of the Mayo Clinic and extracted from clinical guidelines from professional institutions using Gemini 2.5 Pro. For each disease, the average accuracy achieved using these two guideline knowledge sources is established as the Baseline Knowledge. A dataset called MIMIC-MACD (Supplementary Material S1) is constructed, which consists of 4,390 cases sourced from the MIMIC-CDM [9] and the MIMIC-IV v2.2 [39], encompassing seven diseases. Each case includes four categories of information: history of present illness, physical examination, laboratory results, and radiation reports. The entire dataset is partitioned into two subsets: a sampling set, which contains the learning cases for the knowledge self-learning process, and a test set used for final evaluation. All reported experimental results are from the test set, and their performance is characterized using primary diagnostic accuracy.

Experimental results confirm the superiority of the MACD framework, as shown in Fig. 2. The Self-Learned Knowledge it generated consistently leads to higher average accuracy across most tested models compared to the baseline knowledge. When evaluated on seven diseases, the MACD framework improves diagnostic accuracy over the baseline knowledge by 10.3% for Llama-8B, 8.7% for DeepSeek-70B, and 15.8% for Llama-70B, marking an average improvement of 11.6%. This positive effect, though varying in degree, is observed across most individual diseases. We attribute this success to the nature of the Self-Learned

Knowledge; unlike authoritative knowledge curated for human cognition, it contains more clinically specific symptoms and is structured in a way that is inherently more compatible with the LLMs' inferential patterns, thus leading to a more significant improvement in clinical decision making.

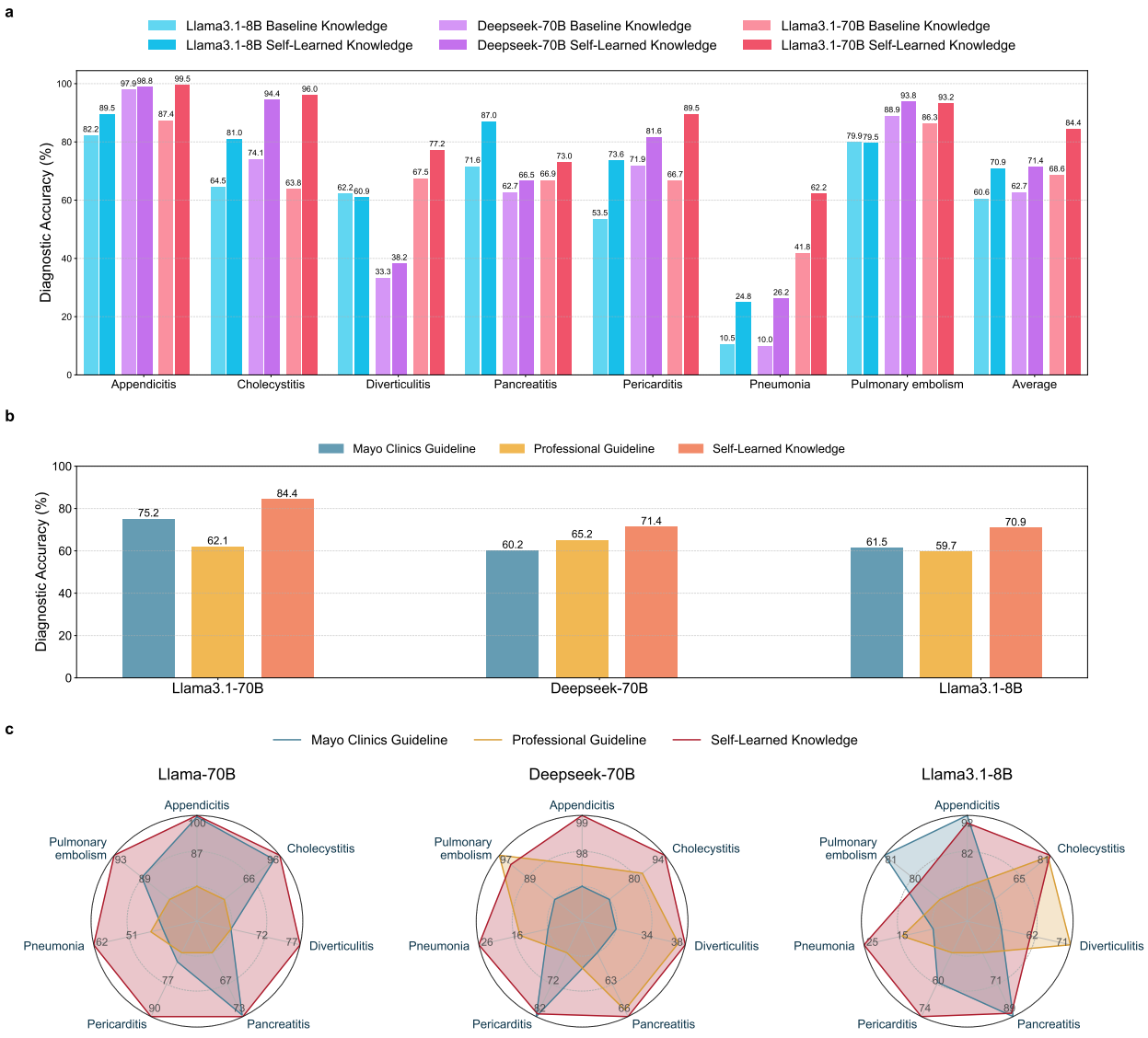

Figure 2: **Comparison of diagnostic accuracy between Self-Learned Knowledge and Baseline Knowledge.** (a) Diagnostician agents using different base models in the Self-Learned Knowledge and Baseline Knowledge. (b) Comprehensive diagnostic accuracy of diagnostician agents based on different LLMs in the Mayo Clinic Guideline, Professional Guideline, and the Self-Learned Knowledge. (c) Diagnostic accuracy of diagnostician agents based on different LLMs in the Mayo Clinic Guideline, Professional Guideline, and the Self-Learned Knowledge for different pathologies.

The MACD Framework Demonstrates General Applicability

The proposed MACD framework demonstrates remarkable generalizability, as validated through three sets of comparative experiments. The results from these experiments show that, compared to their respective baselines, the MACD framework delivers significant and stable improvements in diagnostic accuracy across all tested models and diseases. This consistent performance underscores its broad compatibility and efficacy as a 'plug-and-play' method.

First, we introduce a 'zero knowledge' (Supplementary Material S2), where the diagnostician agent performs diagnosis based solely on its internal parameters, to represent its intrinsic diagnostic capability. The baseline diagnostic accuracy of the diagnostician agent varies as expected, from a low of 42.6% based on Llama-8B to a high of 56.8% based on Llama-70B. Guiding the diagnostician agents with the Self-Learned Knowledge from the agent team yielded substantial improvements for all base models, with accuracy reaching 70.9% for Llama-8B, 71.4% for DeepSeek-70B, and an impressive 84.4% for Llama-70B.

Second, for further validation of these results, the work also compares the performance of the diagnostician agents guided by Self-Learned Knowledge against traditional methods such as Chain-of-Thought (CoT) and few-shot learning, where it again demonstrates a distinct advantage (Supplementary Material S3).

Third, compared with guideline knowledge sources, the Self-Learned Knowledge demonstrates a stronger guiding effect. Compared to the Professional Guideline, MACD framework leads to accuracy improvements in the diagnostician agents of +9.4% (Llama-8B), +11.2% (DeepSeek-70B), and +9.2% (Llama-70B). Similarly, when compared with the Mayo Clinic Guideline, the performance gain from the MACD framework is also pronounced (Llama-8B: +11.2%; DeepSeek-70B: +6.2%; Llama-70B: +22.3%), as shown in Fig. 2b.

A deeper analysis at the individual disease level (Fig. 2c and Supplementary Material S4) reveals a clear model dependency. The diagnostician agents based on the top-performing Llama-3.1-70B surpass both guidelines in all seven diseases, proving that a sufficiently capable base model allows the agent system to achieve a comprehensive advantage. In contrast, this advantage is not absolute for agents based on other models. The DeepSeek-70B-based agent fails to surpass the Mayo Clinic Guideline on pericarditis (81.6% *vs.* 82.5%) and pulmonary embolism (93.8% *vs.* 97.3% from Professional Guideline), while the Llama-8B-based one exhibits the same shortcoming in four diseases. This performance disparity reveals a deeper trend: the stronger the base model's capabilities, the better the agent performs across various diseases.

The Self-Learned Knowledge Manifests Stability and Transferability

In clinical applications, it is crucial that performance improvements from an applied method be traceable. The study proposes that the effects of different knowledge on a diagnostician agent should exhibit two key properties: stability and transferability. We define stability as the principle that when provided with the same authoritative knowledge, performance improvements across different models should align with the

inherent performance trends of the models themselves. Transferability, in turn, dictates that sufficiently authoritative knowledge should yield significant performance enhancements across a diverse range of models. Therefore, to assess these properties, the performance of various diagnostician agents is investigated, each based on a different underlying model, when provided with identical knowledge inputs.

As shown in Fig. 3, the Zero Knowledge reveals a clear hierarchy in the diagnostician agents' intrinsic clinical decision-making capabilities: using Llama-70B, the diagnostician agent is the top performer (56.8% average diagnostic accuracy), followed by DeepSeek-70B (45.9%), with Llama-8B being the weakest (42.6%). To test knowledge stability, an experiment where the Self-Learned Knowledge generated by the top-performing Llama-70B-based agent teams is applied to the other two diagnostician agents is designed.

Firstly, the result finds that conventional guideline knowledge produces inconsistent and unpredictable results across different diagnostician agents. For example, as seen in Fig. 3a, Professional Guideline yields the highest diagnostic accuracy with the DeepSeek-70B-based agent (65.2%) but the lowest with the Llama-8B-based agent (59.7%). Similarly, information from the Mayo Clinic Guideline is the most effective for the Llama-70B-based agent (75.2%) but significantly the weakest for the DeepSeek-70B-based one (60.2%). This erratic behavior demonstrates that the efficacy of standardized, human-designed knowledge is highly uncertain when applied to different LLMs. In stark contrast, when using the Self-Learned Knowledge generated by the MACD framework, the performance of the agents aligns perfectly with their baseline capabilities: the Llama-8B-based agent is the weakest (63.7%), and the Llama-70B-based agent is the strongest (84.4%). As further illustration across various diseases in Fig. 3, this pattern of the Self-Learned Knowledge producing results consistent with the models' intrinsic performance is a consistent trend. This demonstrates that the MACD framework's outputs yield far more stable and predictable performance improvements across models than conventional guidelines.

Secondly, the application of certain Self-Learned Knowledge generated by the MACD framework consistently outperforms both the Mayo Clinic Guideline and the Professional Guideline. Specifically, in Fig. 3a, compared to Mayo Clinic Guideline information, the Self-Learned Knowledge improves the diagnostic accuracy of the diagnostician agents by +2.2% (Llama-8B), +9.2% (DeepSeek-70B), and +8.9% (Llama-70B). The advantage over the Professional Guideline is also clear, with performance boosts of +4.0% (Llama-8B), +4.2% (DeepSeek-70B), and +22.3% (Llama-70B). Compared to the other two guidelines, which are model sensitive and yield unpredictable effects, the Self-Learned Knowledge demonstrates superior cross-model transferability of results. These results strongly suggest that the Self-Learned Knowledge obtained through the MACD framework embodies a more universal and LLM-friendly representation of clinical knowledge.

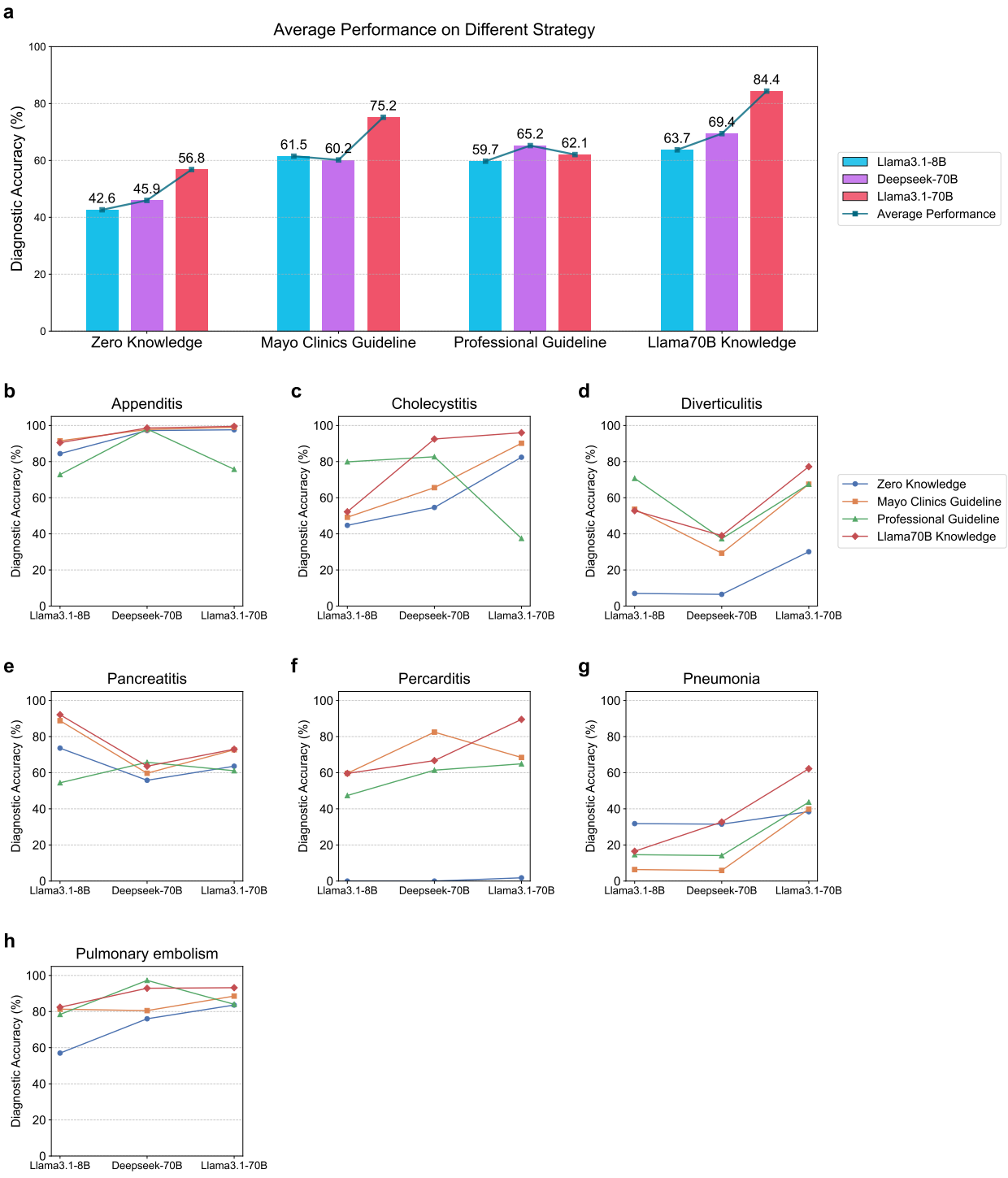

Figure 3: **Self-Learned Knowledge demonstrated greater stability and cross-model transferability.** The Self-Learned Knowledge of the Llama-70B agent team also brings effective performance improvement and demonstrates a performance change trend consistent with the Zero Knowledge.

LLM Prefers Knowledge Learned by Itself

Further investigation into the optimal application strategy for the MACD framework reveals a critical insight: a diagnostician agent exhibits a distinct preference for the Self-Learned Knowledge generated by its own team of knowledge summarizer and knowledge refiner agents. To validate this, the study conducts a transfer experiment where, for a given diagnostician agent, its performance when using its own Self-Learned Knowledge against its performance when using knowledge generated by the other agent-teams' different LLMs is compared.

Each diagnostician agent achieves its peak performance only when using the Self-Learned Knowledge generated by its own agent team, as detailed in Fig. 4a. Even when leveraging the knowledge from the agent team based on the most capable Llama-70B model, its application to diagnostician agents based on weaker models does not yield optimal results. For instance, the accuracy of diagnostician agents based on the Llama-8B model dropped by 7.2% (from 70.9% to 63.7%) when using the Llama-70B knowledge compared to its own. Likewise, the DeepSeek-70B agent's performance is higher with its self-generated knowledge (71.4%) than with the one from Llama-70B (69.4%). This pattern holds true across all combinations, confirming that diagnostician agents consistently perform best with their native, Self-Learned Knowledge.

This phenomenon is attributed to the unique "cognitive styles" of agent teams based on different models. Each model appears to develop distinct patterns for understanding diseases and unique linguistic styles. This creates a comprehension barrier to non-self-learned knowledge, which ultimately degrades diagnostic performance. This hypothesis is substantiated by the content of the Self-Learned Knowledge themselves (Supplementary Material S5), where clear differences in linguistic style and areas of focus among the models are evident upon review, which found significant stylistic distinctions among the knowledge from the three models, with the disparity between Llama-8B and Llama-70B being particularly pronounced. Fig. 4a presents a heatmap showing the semantic similarity between Self-Learned Knowledge generated by agent teams based on different LLMs. This stylistic gap directly correlates with the performance findings, explaining the more significant accuracy drop when applying the Llama-70B knowledge to Llama-8B compared to the more modest decline observed with DeepSeek-70B.

This phenomenon is analogous to the variance in understanding of the same disease among human physicians. In a clinical career, although foundational medical knowledge is universal, different physicians develop distinct understandings of the same diagnostic information. An individual's personalized understanding may not be universally applicable, as this individualized knowledge is most effective for guiding the physician who formed it and is often difficult for others to utilize with the same efficiency.

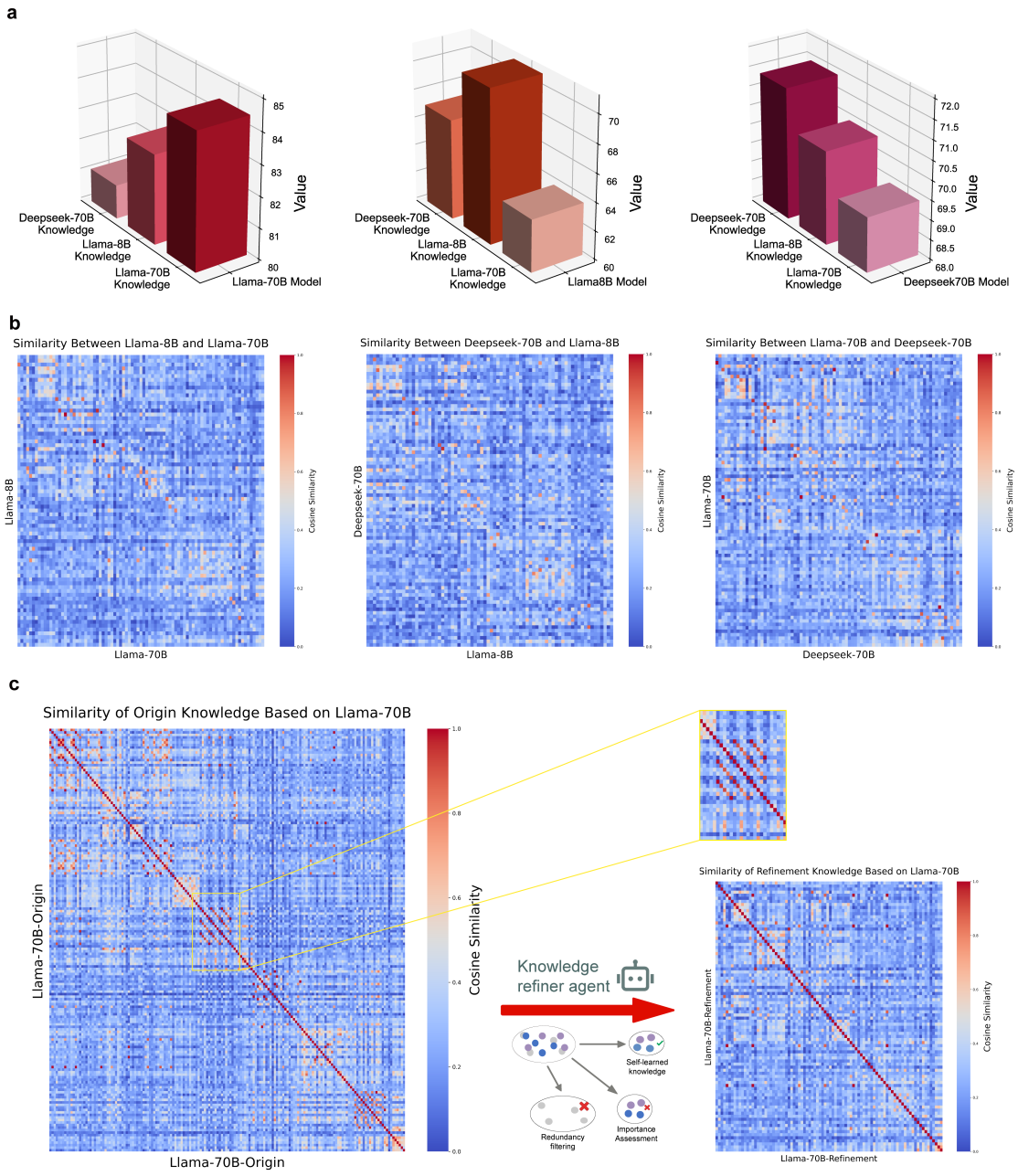

Figure 4: **Diagnostician agents preference for self-learned knowledge generated by its own agent team.** (a) Diagnostic agents can achieve better accuracy by using Self-Learned Knowledge from the same agent team. (b) Displayed a semantic similarity comparison of Self-Learned Knowledge from different agent teams. (c) Semantic similarity comparison of the effects on Self-Learned Knowledge using the knowledge refiner agent.

The MACD Framework Approaches Human Expert-Level Performance

The MACD framework demonstrates statistically significant advantages in diagnostic accuracy and substantial improvements in efficiency when compared with human experts. The MIMIC-MACD-human dataset is constructed by randomly sampling 20 cases from the test set of each disease in the MIMIC-MACD dataset. While prior studies like Hager et al. [9] have noted a significant accuracy gap between LLMs and physicians, the MACD framework elevates the agents' performance to a level that is statistically comparable to, and in many cases superior to, human experts (Table 1). Most notably, the Llama3.1-70B-based agent achieves a diagnostic accuracy that is statistically significantly higher than the human physician benchmark on six of the seven tasks (all $p < 0.01$). Furthermore, it's the only agent whose average accuracy (0.81) is also statistically significantly superior to the human average (0.65, $p < 0.001$), highlighting the framework's robust potential. In cases where superiority is not statistically established, the diagnostician agents perform on par with the expert benchmark, showing no significant difference ($p > 0.05$). In terms of efficiency, the advantage remains stark, with an average time of 13.29 seconds per case compared to 209.71 seconds for human physicians.

A case-by-case analysis of diagnostic patterns also reveals a shared cognitive bias: human physicians often misdiagnose patients with pancreatitis as having cholecystitis or a related condition, a pattern that is mirrored by the diagnostician agents. This demonstrates a similar diagnostic preference between the agents and their human counterparts.

Table 1: Comparison of diagnostic accuracy between physicians and diagnostician agents on sub datasets

LLM / Physicians	Appendicitis	Cholecystitis	Diverticulitis	Pancreatitis	Pericarditis	Pneumonia	Pulmonary embolism	Average Accuracy	Average time(s)
Physicians	0.900	1.000	0.550	0.250	0.250	0.700	0.900	0.650	209.71
Llama3.1 -8B	0.900^{ns}	0.750^{**}	0.600^{ns}	0.750^{**}	0.700^{**}	0.250^{**}	0.750^{**}	0.670^{**}	7.03
DeepSeek -70B	1.000^{**}	1.000^{ns}	0.440^{**}	0.550^{**}	0.700^{**}	0.230^{**}	0.900^{ns}	0.690^{ns}	12.10
Llama3.1 -70B	1.000^{**}	0.950^{**}	0.750^{***}	0.600^{**}	0.900^{**}	0.550^{**}	0.900^{ns}	$\mathbf{0.810}^{***}$	13.29

Note: P-values are calculated using the Wilcoxon Signed-Rank test, a non-parametric method chosen for its robustness with small sample sizes and data not assumed to be normally distributed. Each agent's performance is compared against the corresponding Human Physician result.
Significance levels are denoted as follows: *** $p < 0.001$; ** $p < 0.01$; ^{ns} (no-significant) $p > 0.05$

Table 2: Comparison of diagnostic accuracy between different diagnostic agents and each physician

Human	Accuracy	Llama3.1-8B	DeepSeek-70B	Llama3.1-70B
Physicians-1	0.63	0.57	0.68	**0.79**
Physicians-2	0.50	0.75	0.75	**0.85**
Physicians-3	0.60	0.65	0.65	**0.80**
Physicians-4	0.65	0.60	0.55	**0.70**
Physicians-5	0.70	**0.70**	**0.70**	0.65
Physicians-6	0.67	0.57	0.61	**0.81**
Physicians-7	0.74	**0.94**	0.68	0.79

Self-Learned Knowledge Outperforms Guidelines in MACD-Human Collaboration Workflow

To further assess the impact of different knowledge sources in a collaborative reasoning context, the MACD-human collaboration workflow is implemented as a medical consultation system to provide effective opinions for human physicians. The evaluation focuses on two key metrics: the effective opinion rate, which measures the proportion of the three diagnostician agents that provide correct diagnostic results (detailed in Evaluation Metrics in Methods), and the rate of diagnostic consensus achieved by the collaboration workflow through iterative rounds of analysis. The framework's performance is evaluated under the guidance of three distinct types of knowledge: the Self-Learned Knowledge, the Mayo Clinic Guideline, and the Professional Guideline. The results demonstrate that the Self-Learned Knowledge holds a significant advantage in all metrics. Furthermore, three human physicians are invited to independently validate the effectiveness of the opinions generated by the workflow on the MIMIC-MACD-human dataset. They provide further diagnostic assessments for cases where the collaboration workflow fails to reach consensus, based on the model's outputs, ultimately determining the final diagnostic results (detailed in MACD-Human Collaboration Workflow in Methods). The diagnostic accuracy encompasses both the correct results from cases where the collaboration workflow reaches consensus and the final diagnostic outcomes determined by human experts.

The Self-Learned Knowledge demonstrates the most efficient initial consensus. The study analyzes the diagnostic consensus rate to measure how quickly agents converge on a diagnosis. In the initial round of discussion, the framework guided by the Self-Learned Knowledge resolves the highest consensus rate, with 58.6% rate. This surpasses the initial agreements achieved using the Professional Guideline at 50.1% and Mayo Clinic Guideline at 49.3% (Fig. 5a). While the performance gap narrows in subsequent rounds with cumulative agreements becoming highly comparable by the third round (74.5% for the Self-Learned Knowledge, 74.3% for Mayo Clinic Guideline, and 73.5% for Professional Guideline), the initial efficiency advantage of the Self-Learned Knowledge is evident.

The Self-Learned Knowledge leads to the highest effective opinion rate, providing more valuable reference results for human physicians. The framework utilizing the Self-Learned Knowledge achieves a superior rate of

88.5% in Fig. 5b. This performance is markedly higher than that of the framework guided by the Professional Guideline (83%) and Mayo Clinic Guideline (79.3%).

The diagnostic accuracy of human physicians with the collaboration workflow on the MIMIC-MACD-human dataset is validated. When employing the Self-Learned Knowledge, the average diagnostic accuracy across seven diseases reaches 83.6%, surpassing both Mayo Clinic Guidelines (76.7%) and Professional Guidelines (77.1%), thereby achieving superior performance. At the individual disease level, self-learned knowledge achieves equal or superior performance compared to the other two guidelines across six diseases, as illustrated in Fig. 5c.

Furthermore, when utilizing self-learned knowledge, the collaboration workflow outperforms both human physicians alone and the strongest single diagnostician agent, demonstrating that the collaboration workflow possesses significant practical clinical application value(0.836 for the workflow, 0.810 for diagnostician agent based on Llama3.1-70B, and 0.650 for physicians), as illustrated in Table 3. This superior performance underscores the framework's potential for real-world medical diagnostic scenarios, where the integration of self-learned knowledge with collaborative multi-agent clinical diagnosis can enhance diagnostic accuracy beyond traditional guideline-based approaches.

Table 3: Diagnostic accuracy of physicians, diagnostician agents and MACD-human collaboration workflow

LLM / Physicians	Appendicitis	Cholecystitis	Diverticulitis	Pancreatitis	Pericarditis	Pneumonia	Pulmonary embolism	Average Accuracy
Physicians	0.900	**1.000**	0.550	0.250	0.250	**0.700**	0.900	0.650
Llama3.1 -70B	**1.000****	0.950**	0.750***	0.600**	0.900**	0.550**	0.900$^{\text{ns}}$	0.810***
MACD-human collaboration workflow	**1.000****	0.983$^{\text{ns}}$	**0.833****	**0.717****	**0.917****	0.467**	**0.933**$^{\text{ns}}$	**0.836*****

Note: P-values are calculated using the Wilcoxon Signed-Rank test, a non-parametric method chosen for its robustness with small sample sizes and data not assumed to be normally distributed. Each agent's performance is compared against the corresponding Human Physician benchmark.
Significance levels are denoted as follows: *** $p < 0.001$; ** $p < 0.01$; $^{\text{ns}}$ (no-significant) $p > 0.05$

The MACD Framework Affords Explainability in the Diagnostic Process

To enhance the transparency and trustworthiness of the diagnostician agents' diagnostic process, MACD framework incorporates an explainability design, which primarily consists of two aspects: causal intervention on Self-Learned Knowledge and the output of diagnostic rationale. As part of the knowledge refiner agent's workflow, the study employs a concept-based causal intervention method (Multi-Agent Clinical Diagnosis Framework in Methods), quantifying the impact of each piece of Self-Learned Knowledge on the final diagnostic accuracy by systematically removing them one by one for a specific disease. Fig 4 presents the results for the knowledge refiner agent based on different models (Supplementary Material S5 and Supple-

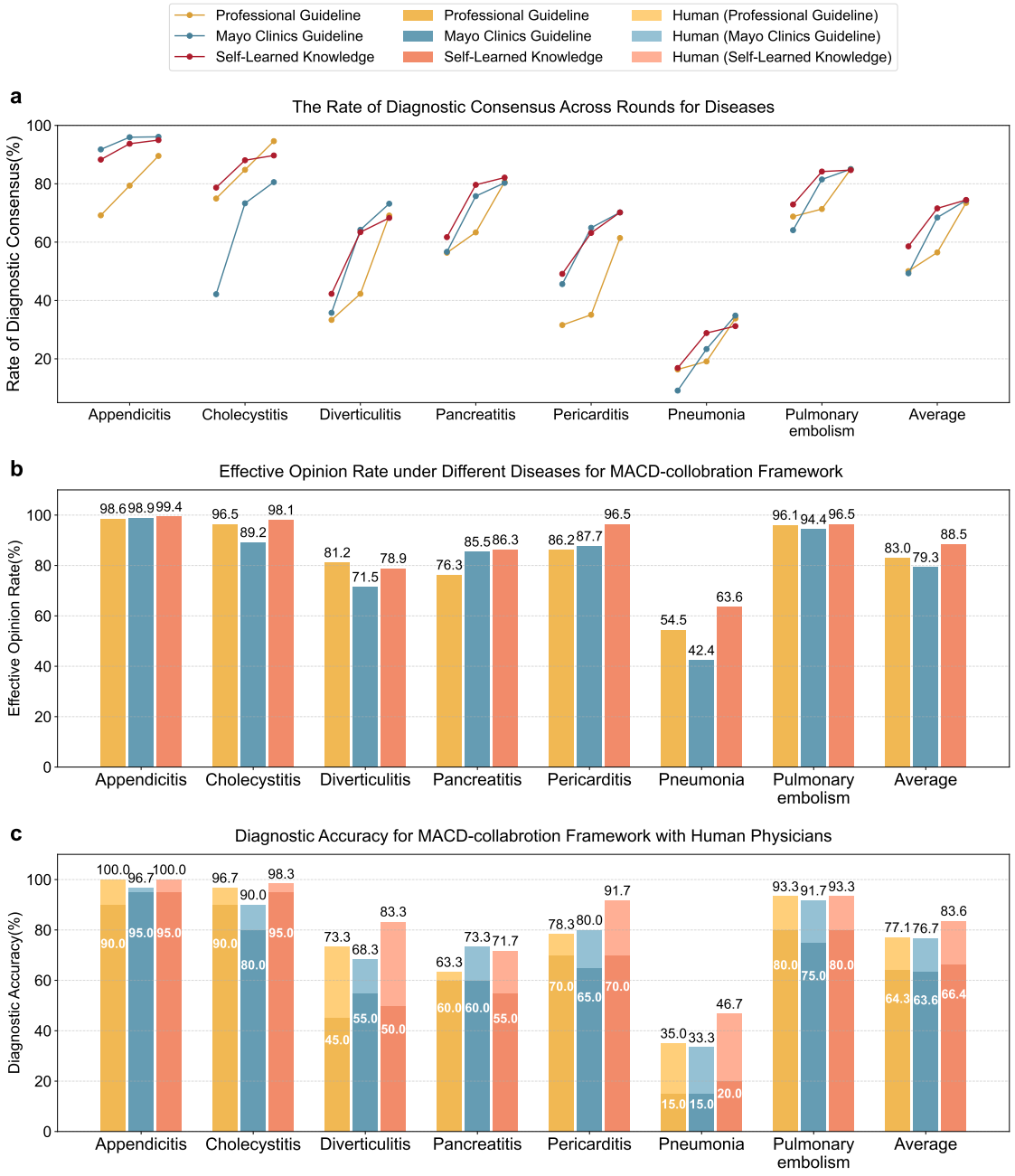

Figure 5: **The MACD-human collaboration workflow achieves higher diagnostic accuracy and faster consensus with Self-Learned Knowledge.** (a) The proportion of cases with different knowledge types that reach consensus within the first three rounds of comparison is shown. Self-learned knowledge achieves the highest initial diagnostic consensus rate. (b) The rate of effective opinion provides to human physicians using different external knowledge sources is shown, with self-learned knowledge yielding the best performance. (c) Diagnostic accuracy of human physicians on the MIMIC-MACD-human dataset when assisted by different knowledge sources, with self-learned knowledge achieving the best results.

mentary Material S6) , where the result finds that removing three concepts with a negative impact on the diagnosis of diverticulitis improves the accuracy of Llama-70B by 3.5% (detailed in Supplementary Material S6.3). This method not only facilitates the identification and optimization of the Self-Learned Knowledge content but also provides an explorable basis for understanding the decision-making process of the agents.

Furthermore, the experiment requires the diagnostician agents to explicitly output the diagnostic criteria alongside the final diagnosis. In contrast to 'black-box' solutions that only provide a diagnostic result, this textual decision pathway significantly enhances the traceability of the process and the explainability of the final output. Some typical output examples are shown in Fig. 6. For a given case, the MACD framework not only provides the diagnostic agent with Self-Learned Knowledge as an aid for diagnosis, but also fully transparently displays the rationale for the agent's conclusion in the final output. This rationale is closely linked to both the original case content and the provided Self-Learned Knowledge, demonstrating a clear and traceable basis for the diagnostic decision.

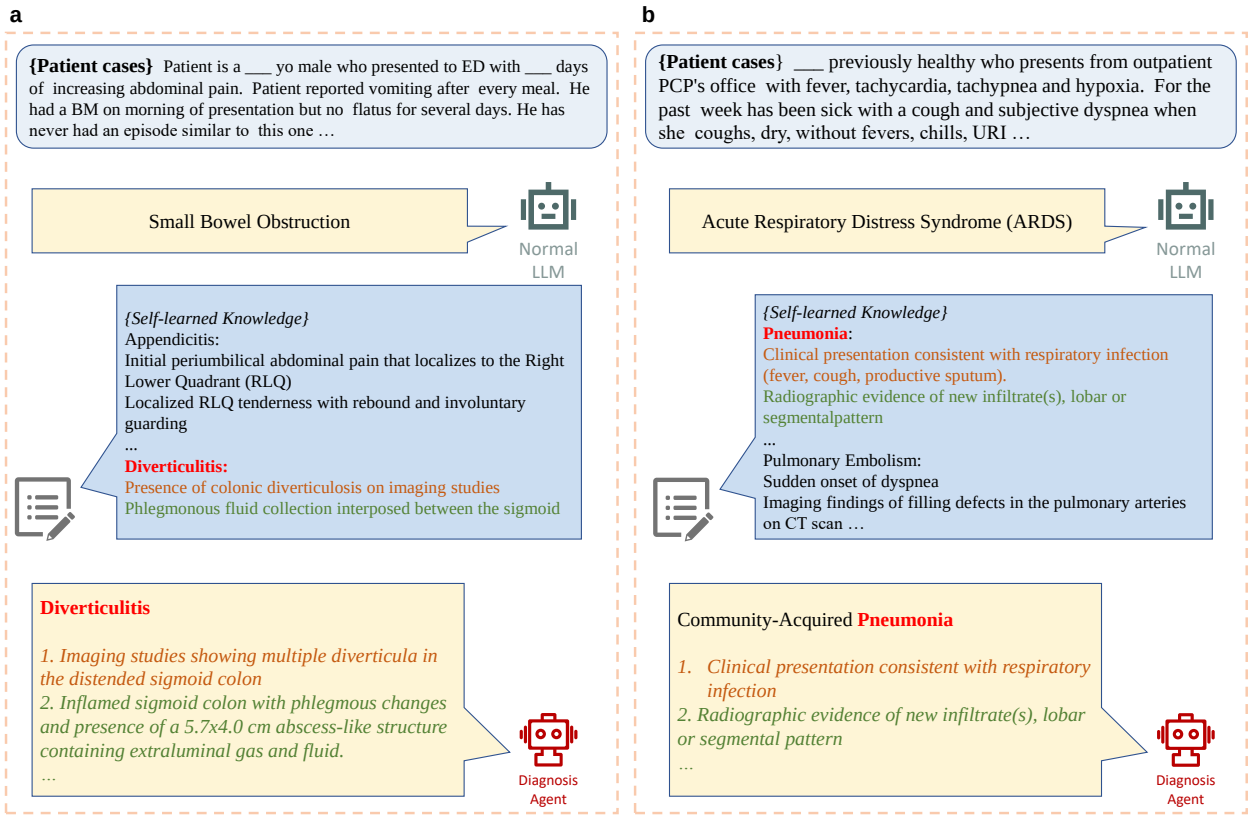

Figure 6: **MACD explicitly output the diagnostic criteria alongside the final diagnosis.** (a) Demonstrates its performance in abdominal diseases. (b) Demonstrates its performance in chest diseases.

Discussion

This study introduces and validates the MACD framework designed to simulate the experience accumulation process of human clinicians. By operationalizing this simulation through a team of specialized agents, the framework significantly enhances the diagnostic accuracy of diagnostician agents in complex clinical tasks, demonstrating excellent universality across different agent architectures. The core contribution lies in proposing an effective pathway to bridge the gap between the vast general medical knowledge of LLMs and the nuanced demands of clinical practice. This gap arises because, although LLMs excel in general medical knowledge, their application to specific, complex clinical scenarios remains challenging; studies [40, 41, 9, 42] consistently highlight limitations in their accuracy, consensus, and reasoning abilities in such contexts.

The innovation of this framework lies in the fact that it does not simply force-feed knowledge into the LLM; instead, it simulates the core process by which clinicians accumulate practical experience, thereby establishing a personalized experience repository for the diagnostic agent. The framework guides the knowledge distillation agent to autonomously distill and categorize diagnostic concepts from actual clinical cases. Its work goes beyond extracting high-frequency features (e.g., "RLQ pain" for appendicitis and "Elevated serum lipase level, $>$ 3 times upper limit of normal" for pancreatitis); it also captures clinically indicative subtleties often omitted from formal guidelines (for instance, the Self-Learned Knowledge for pancreatitis included "History of recent heavy ethanol consumption" as a potential cause). This initial step explicitly supplements and reinforces the model's semantic understanding of key disease features, fostering a multi-layered cognition of the disease.

Next, the knowledge refiner agent takes on the role of an experienced specialist, simulating the process of lifelong reflection and knowledge consolidation. This agent receives the broad set of concepts from the distillation agent and subjects them to a rigorous critique. In the Multi-Agent Clinical Diagnosis Framework, it employs a dual-filter mechanism based on redundancy and importance. By removing repetitive and misleading entries and using the concept-based causal intervention method to quantify the actual impact of each concept on the diagnosis, the agent ultimately retains a set of Self-Learned Knowledge that is highly optimized, refined, and tailored to its LLM's own thinking pattern. This mechanism effectively helps the diagnostic agent anchor on key information when encountering new cases, enabling it to better address the misalignment between its inherent medical knowledge and actual clinical practice.

A key finding of the work is that the Self-Learned Knowledge generated by the MACD framework is significantly superior in enhancing diagnostic performance compared to the guidelines knowledge formulated by human experts. This does not negate the authority of the guidelines but rather reveals an issue of suitability regarding the knowledge format. Although the Professional Guideline and information from the Mayo Clinic Guideline are clinical theories distilled by human experts from extensive practical experience, their primary purpose is to serve as a reference for humans. Their linguistic structure, logical hierarchy,

and key information are tailored to human cognition and workflows. For example, for pancreatitis, the guidelines' description of imaging focuses on examination modalities and severity grading. For diverticulitis, while the guidelines mention its radiological signs, the description is more concentrated on disease staging based on imaging results. For an LLM-based agent, such external knowledge requires further interpretation and analysis, which may lead to comprehension biases and a loss of efficiency in its application. The MACD framework guides the LLM-based agent to autonomously summarize from real-world cases, and the resulting Self-Learned Knowledge incorporates the LLM's own individualized understanding and specific representations of the clinical data. This self-generated knowledge, in its linguistic style and logical structure, is highly compatible with the diagnostic agent internal reasoning mechanisms, making its application naturally more direct and effective. In contrast to information from guidelines that requires further analysis by the agent, the Self-Learned Knowledge directly distills radiological descriptions that are more easily comprehended by the LLM (e.g., "CT scan showing pancreatic inflammation" for pancreatitis). To validate the credibility of the content produced by the MACD framework, the study introduces an evaluation by human physicians regarding the Self-Learned Knowledge's clinical diagnostic relevance, further verifying its clinical value.

Furthermore, this work observes that each agent team's preference for self-learned knowledge reveals an individualized characteristic of its own experience, a phenomenon we term agent-specific individuality. Agents build on different LLMs, owing to variations in their architecture and training data, and may develop unique thinking patterns. They are more adept at understanding and applying information synthesized and refined by their own teammates, whereas for external information, even from a more capable agent team, differences in style and perspective can create a comprehension barrier. This suggests that the most effective path for future clinical LLM applications may not be to build a single, massive, universal knowledge base, but rather to empower each agent system to learn continuously from specific data, thereby forming its own personalized and dynamically evolving repository of experience.

Compared with existing solutions, such as novel prompt structures or parameter fine-tuning to enhance medical knowledge comprehension [43], the MACD framework is conceptually distinct and exhibits unique advantages. First, unlike prompting methods that focus on optimizing the reasoning process (e.g., CoT [44], RoT [45], ToT [46], self-refine [18]), the true value of the framework lies in building a long-term, reusable, and growing accumulation of experience. We do not optimize the model's single inference process; instead, through the accumulation of experience, we continuously narrow the gap between the model's medical knowledge and actual clinical cases, allowing it to learn autonomously in practice in a way that more closely aligns with the growth trajectory of a human expert. Second, compared to solutions that rely on parametric fine-tuning to inject domain knowledge, framework is more lightweight, flexible, and secure. Fine-tuning methods implicitly and permanently encode knowledge into the model's weights, a process that is costly and difficult to update [43]. In contrast, the framework injects knowledge explicitly and dynamically via

prompting. This not only significantly lowers the technical barrier and practical costs but also endows the system with updatability and interpretability, as the accumulated experience can be iterated upon by learning from new, human-readable cases. More importantly, this model allows data processing and updates to be completed locally, providing a feasible solution to the data privacy challenges in medical LLM.

Despite the positive results of this study, several limitations remain. First, while the current MACD framework relies on a structured, manually-guided workflow, it proves effective in the diagnostic process. This provides a foundational concept and sets a precedent for the development of more sophisticated, fully-automated agent systems. Second, regarding the data, the MIMIC-IV dataset is predominantly text-based. The medical reports within it are written by human physicians, meaning the information is pre-processed and may be subject to human bias. In real-world clinical scenarios, however, physicians supplement their analysis by directly interpreting medical images. Therefore, enabling LLMs to directly process imaging data could potentially enhance their understanding of key patient information. Thirdly, the MIMIC-IV dataset is primarily in English and sourced from the United States. It remains unclear whether the framework can achieve similarly excellent performance on medical data from other countries and regions, and further validation with more diverse clinical data is required.

The method proposed in this study opens up new possibilities for the application of LLMs in clinical diagnosis, and future work can be expanded in the following directions. First, the work evaluates the MACD-human collaboration workflow based on whether at least one agent provides the correct diagnosis, as the results are intended to serve as a reference for human physicians. A deeper investigation is warranted into how the Self-Learned Knowledge can be optimally leveraged within the collaborative consultation setting to maximize the framework's full potential. Additionally, the current MACD framework provides a viable approach for accumulating diagnostic experience. This work demonstrates its feasibility across multiple diseases, showing that knowledge accumulation enhances the model's diagnostic performance across diverse conditions. The framework holds promise for advancing LLMs' diagnostic capabilities in specialized disease areas, potentially contributing to more accurate and focused specialty-specific diagnosis in the future. Finally, the medical diagnostic process involves complex ethical and safety issues. The interpretability of current LLMs within this process requires further advancement to achieve a level of trustworthiness acceptable to both clinicians and patients. Also, it is important to note that even though the MACD framework achieves results surpassing human experts in the data, this does not imply its immediate readiness for direct clinical application.

This study successfully constructs and validates a novel multi-agent clinical diagnosis framework (MACD framework). By simulating the experience accumulation process of human physicians, this framework effectively improves the accuracy and generalizability of LLMs in open-ended clinical diagnostic tasks, bringing their performance to a level that approaches and, in some cases, surpasses that of human experts. We have

not only demonstrated the immense potential of LLMs in complex clinical reasoning but, more importantly, by making their learning process more transparent and aligned with human clinical logic, the framework provides a promising and innovative path toward enhancing the trustworthiness and interpretability of LLMs in medical applications. We believe that with continuous technological advancement and further in-depth validation, this approach centered on simulating and enhancing clinical experience will significantly advance the real-world deployment of LLMs in the healthcare domain, ultimately benefiting patients worldwide.

Methods

Dataset Construction

The dataset for the study is called MIMIC-MACD, which is constructed based on the MIMIC-IV v2.2 database and combines two specialized clinical decision datasets, totaling 4390 patient cases across seven abdominal and thoracic diseases. The data distribution is detailed in Supplementary Matrial Dataset Composition. The first, the MIMIC-CDM dataset from the work of Hager et al. [9], contains 2400 real-world cases of emergency abdominal pain, covering four common abdominal diseases: Appendicitis (n=957), Cholecystitis (n=648), Diverticulitis (n=257), and Pancreatitis (n=538). To further validate the generalizability of the MACD framework across different clinical domains, we created a new chest disease dataset, following the construction principles similar to those of MIMIC-CDM. This dataset comprises 1,990 cases covering three key thoracic diseases: Pneumonia (n=1024), Pulmonary Embolism (n=852), and Pericarditis (n=114). All cases adhere to a uniform data structure, providing the model with de-identified textual information from four key sections: History of Present Illness, Physical Examination, Laboratory Results, and Radiology Reports.

The MACD framework aims to enhance performance through the autonomous summarization of Self-Learned Knowledge by the agent teams, rather than relying on traditional supervised fine-tuning. Nevertheless, a subset of samples is still required for this learning process. To prevent data leakage from overlapping sampling and testing samples, we partition each disease dataset into a Sampling Set and a Test Set. This process involves the following steps: first, we have the three diagnostician agents, which, based on Llama-3.1-8B, Llama-3.1-70B, and DeepSeek-R1-Distill-Llama3.3-70B respectively, perform an initial round of direct, open-ended diagnosis on the entire cohort of cases. For each disease, we pool all cases that are correctly diagnosed by at least one of the diagnostician agents to create a learning cases pool. Next, from this pool, we perform separate random sampling for each agent team to generate its own exclusive set of learning cases. In practice, while the number of learning cases is nearly identical for each agent team, the specific cases within each set differ substantially from those of the other teams. The union of the learning cases from all agent teams constitutes the Sampling Set, and the remaining cases are allocated to the Test Set. Due to the high diagnostic difficulty of pericarditis, which results in fewer initial correct diagnoses by the diagnostician agents, a uniform number of 23 learning cases is selected for all three models for this specific disease to ensure fairness.

It should be emphasized that, during the knowledge summarizer agent, each LLM uses only its exclusive set of learning cases to generate its Self-Learned Knowledge. Upon manual review, these learning cases are generally found to have more typical characteristics and clearer diagnostic clues, which help the LLMs to learn and distill diagnostic patterns more efficiently. Subsequently, we evaluate the change in each LLM's

performance on the more clinically complex Test Set after applying its self-generated Self-Learned Knowledge.

Model Selection and Deployment

This work selects three general-purpose LLMs as the base model of the MACD framework: Llama-3.1-8B, Llama-3.1-70B, and DeepSeek-R1-Distill-Llama3.3-70B. The rationale for their selection is threefold: (1) They all belong to advanced open source model series and have demonstrated excellent performance on various benchmarks. (2) They differ in parameter scale and training strategies, which provides a basis for evaluating the robustness and effectiveness of the MACD framework on models with varying reasoning capabilities. (3) The models are of a size that is conducive to local deployment.

To ensure the consistency of the experimental results, specific deployment parameters are configured for the models. The context window is limited to 16384 tokens. Additionally, the temperature is set to 0.01, top-k to 1, and top-p to 0.05. All experiments are conducted on NVIDIA A100-80G GPUs.

Construction of Clinical Guideline

To compare the Self-Learned Knowledge autonomously generated by the models with guideline knowledge, we construct two types of baselines based on clinical guidelines. We construct the Mayo Clinic Guideline Baseline Knowledge by manually extracting relevant diagnostic information for each target disease from the Diseases & Conditions directory of the official Mayo Clinic Guideline website. For each disease, the complete information from the overview, symptoms, and diagnosis sections is compiled. This extracted content is then directly integrated into the prompt and provided to the LLM as one of the guideline knowledges (Supplementary Material S7).

We collect clinical practice guidelines published by several authoritative international medical organizations, including the World Society of Emergency Surgery (WSES), the European Society of Cardiology (ESC), and the European Respiratory Society (ERS). Given that the original guideline documents are lengthy and information-dense, we employ the Google Gemini 2.5 Pro (preview) model to process them. Through specific prompt instructions (detailed in Supplementary Material S8), we direct the model to precisely summarize only the diagnostic information relevant to the target diseases, strictly constraining it from adding any of its own knowledge. This process generates a highly focused Professional Guideline knowledge that remains faithful to the original content (Supplementary Material S9).

Multi-Agent Clinical Diagnosis Framework

The multi-agent clinical diagnosis (MACD) framework is composed of two knowledge agents and a diagnostician agent (Supplementary Material S10). The knowledge summarizer agent autonomously reviews learning cases to generate a broad pool of diagnostic concepts for a specific disease. The knowledge refiner agent then

processes this pool, filters it for redundancy and importance to yield the final, and optimizes Self-Learned Knowledge. For the final diagnosis, this knowledge is provided to either a single diagnostician agent or, for more complex reasoning, the MACD-human collaboration workflow as a form of internal knowledge when diagnosing new cases. This provides clear, experience-based guidance for the agent's reasoning process, directing it to focus more precisely on the key features of the disease and thereby improving the accuracy of the final diagnosis.

The diagnostician agent simulates the process of a clinician making a diagnosis based on medical reports, wherein the agent analyzes the patient's medical report information to derive a primary diagnosis and its supporting rationale. We utilize the diagnostic evaluation framework developed by Hager et al. [9] as the foundation for interacting with all selected models. In the standard diagnostic workflow, the textual information from four sections of each case: history of present illness, physical examination, laboratory results, and radiology reports, is consolidated and provided as input to the agent. The prompt requires the diagnostician agent to output the key evidence (diagnostic criteria) supporting its diagnosis to enhance the process's traceability. The information constituting the diagnostic rationale is derived by the agent itself, which mines key information from the patient's medical reports. Compared to an approach that only outputs the final diagnosis, this agent utilizes a prompt template to guide the LLMs in producing structured output (Supplementary Material S11), which effectively enhances the traceability of the diagnostic process and the interpretability of the agent's output.

As for the knowledge summarizer agent, we guide the agent to process the key information within the learning cases through carefully designed prompt instructions. We guide the agent to process the key information within the learning cases. In this process, the agent autonomously learns and summarizes, forming structured diagnostic concepts. These concepts constitute the agent's internal representation of the diagnostic logic for a specific disease, its key clinical features, and their associations. The agent's behavior during this process is constrained by a prompt template structured as a 5-tuple (Supplementary Material S12).

Next, to improve the quality and efficiency of the generated knowledge, we design a dual-filter knowledge refiner agent based on redundancy and importance, detailed as follows. This method first removes repetitive or highly similar diagnostic concepts to preserve semantic diversity. Then, through an importance assessment, it eliminates concepts that could mislead or negatively impact the diagnosis. This dual-filtering process results in a final set of Self-Learned Knowledge that are efficient, reliable, and tailored to the model itself.

(1) Redundancy Filtering. Since the diagnostic concepts are extracted from numerous past cases, features often overlap between different cases of the same disease. To address this, we perform a de-duplication operation. The approach implements concept de-duplication using BioBERT's semantic embedding method [47]. Specifically, by calculating the cosine similarity, $Sim(c, c')$, between concept vectors, we employ a

greedy algorithm based on maximal marginal relevance to iteratively select candidate concepts that are most semantically distinct from those already chosen, resulting in the set of retained diagnostic concepts. This process is applied separately to both the common and rare concept sets to ensure the comprehensiveness of the diagnostic knowledge.

(2) Importance Assessment. For the concepts retained after redundancy filtering, we implemented a concept-based causal intervention scheme. The retained set may still contain erroneous or spurious concepts that could negatively affect the diagnostician agent. To address this, this knowledge refiner agent sequentially ablates each existing diagnostic concept on the All Cases dataset. It then measures the change in the diagnostic accuracy of the diagnostician agent for the target disease (ΔAcc) when the concept is present versus absent, thereby capturing the impact of each concept on the outcome. If removing a concept causes accuracy to drop, it is labeled a positive concept; if accuracy improves or stays the same, it is a negative concept. We remove the negative concepts with the most significant adverse impact. The remaining concepts then form the final Self-Learned Knowledge for each target disease (Supplementary Material S5 and S13).

Finally, the filtered Self-Learned Knowledge is injected into the prompt template of the diagnostician agent. The model receives this knowledge as prior information before accessing the patient's case data and then proceeds with the diagnosis, thereby achieving the enhancement of its diagnostic knowledge.

MACD-Human Collaboration Workflow

To emulate the collaborative nature of real-world clinical consultation, we develop a MACD-human collaboration workflow (Supplementary Material S10). This architecture is built upon three distinct diagnostician agents and one evaluator agent, simulating the process in which multiple physicians conduct a consultation and reach a consensus diagnosis. The framework is designed to function as a medical assistant, providing effective opinions for a human physician's actual diagnostic process. Through a simulated process of consultation and discussion, the three diagnostician agents analyze a case, collect each other's opinions for more analysis, and iterate until a consensus is reached or a maximum number of discussions is met. The evaluator agent assesses whether the three diagnostician agents have reached agreement after each round of discussion. A foundational principle of this framework is that each agent operates using its own unique, self-generated Self-Learned Knowledge, thereby preserving the model-specific knowledge individuality identified in the experiments (Supplementary Material S14).

The diagnostic process is governed by the evaluator agent with a collaborative and iterative strategy detailed in the 'Evaluation Metrics'. In each discussion, the three diagnostician agents first diagnose a case independently, and their results are then assessed by the evaluator agent. If a consensus is not met, the case, along with all conflicting diagnostic results, automatically proceeds to the next diagnostic loop. In each subsequent discussion, all diagnostician agents are provided with an enriched informational context, which

includes the anonymized diagnostic outputs from the previous round. This loop continues until a consensus is reached or a predefined maximum number of discussions is met. For cases that achieve consensus, the agreed-upon result serves as the final output. If no consensus is reached, the diagnostic results from the final round are provided as the ultimate effective opinions; these diagnostic results are then submitted to human physicians for the final diagnosis.

Evaluation Metrics

We adopt a hierarchical evaluation strategy to quantitatively analyze diagnostic accuracy. For single-agent performance, we apply a two-level matching system. At the first level, a diagnosis is considered correct if the model's output contained the core medical term for the target disease (exact term matching), ignoring any modifying adjectives. To account for common terminological variations found in clinical practice, we design a secondary, more tolerant matching rule based on anatomical location. This rule accepts reasonable inferences within the same organ system (e.g., accepting "pericard effusion" as a tolerantly accurate diagnosis for "pericarditis") and permits modifying adjectives related to disease severity (Supplementary Material S15). Building on the work of Hager et al.[9], add tolerant matching rules for pericarditis, pneumonia, and pulmonary embolism, all of which are reviewed and approved by human experts. The experimental results for single-agent performance in this paper are reported as the top-1 accuracy based on the exact term matching criterion.

In addition to single agent accuracy, the study establishes a collaboration evaluation strategy to adjudicate consensus within the MACD collaboration framework. This consensus assessment transcends simple string matching to achieve a more clinically meaningful measure of agreement and comprises a two-stage process. First, all raw diagnostic results from the agents are processed using the tolerant name-matching rules described previously. This step normalizes clinically equivalent terms into a core medical term for the target disease while preserving non-conforming diagnostic terms in their original form. Following this standardization, the diagnoses are subjected to a semantic similarity analysis using the BioBERT model. A consensus among all diagnoses is confirmed only if their pairwise cosine similarity score surpasses a predefined threshold. This dual methodology ensures that only diagnoses that are truly semantically aligned are considered concordant, providing a robust and reliable method for adjudicating agreement. Finally, to evaluate the clinical utility of the framework's final output, the effective opinion rate is introduced, which is calculated as the proportion of total cases for which the framework provided an effective opinion. The output for a given case is deemed 'effective' only if the correct target disease is mentioned at least once in the diagnostic results provided by the collaborative framework; otherwise, the output is considered 'ineffective'.

Reader Study

To establish a human expert performance baseline, seven Emergency Medicine attending physicians with professional experience ranging from 3 to over 20 years are recruited to participate in the diagnostic study. The physicians are divided into two specialized groups: a group of three physicians is responsible for diagnosing the chest disease cases, and a group of four physicians is responsible for the abdominal disease cases. The cases within each category are distributed equally among the physicians in the respective group. The evaluation primarily covers the following three aspects.

Human experts are invited to evaluate the medical reliability of the Self-Learned Knowledge. Six of the seven participating physicians independently scored each Self-Learned Knowledge generated by the three different LLMs. The core of the evaluation is to assess the strength of association between each concept in the knowledge and its target disease. A 5-point Likert scale is used for scoring (Supplementary Material S16). Finally, the average score from all physicians for all concepts generated by a single model is calculated to serve as the overall relevance score for that model's knowledge (Supplementary Material S17).

The goal is to establish a reliable reference standard for LLM performance based on the diagnostic capabilities of human physicians. The physicians are required to independently diagnose a randomly sampled subset of cases, which consists of 80 abdominal cases (20 for each of the four diseases) and 60 thoracic cases (20 for each of the three diseases). To ensure fairness, the case information and the list of possible disease types provided to each physician are identical to those given to the LLMs. The case information includes the History of Present Illness, Physical Examination, Laboratory Results, and Radiology Reports. Based on this information, the physicians are asked to provide their most likely primary diagnosis. To prevent physicians from identifying disease patterns, we include an additional 20 abdominal and 15 chest cases of other related diseases as distractor cases. Consequently, each physician in the respective groups evaluates a total of 100 abdominal or 75 thoracic cases. All cases are provided through a website made by ourselves (Supplementary Material S18), with the content and presentation format being identical to that given to the LLMs, and the case order is fully randomized. After all physicians complete their diagnoses independently, we calculate the average diagnostic accuracy across the group to serve as the final human expert performance baseline.

Code availability

The code is openly available data, the following link for non-commercial purposes: `https://github.com/qjdzj/MACD`. All LLM prompts are included in the Supplementary Material with the prompts used.

Data availability

Dataset is openly available at the following link for non-commercial purposes: `https://github.com/qjdzj/MACD`

Acknowledgements

We would like to express our gratitude to Xin Li for his contributions in the presentation of experimental data, provision of medical references, and proofreading of article content. Thank you for Chunjiang Wang's comments on the description of the supplementary materials section.

This work is supported by the Natural Science Foundation of China under Grants 62271465, 62402473, the Suzhou Basic Research Program under Grant SYG202338, Jiangsu Funding Program for Excellent Postdoctoral Talent, and the China Postdoctoral Science Foundation under Grant 2024M763178.

Author Contributions

W.L., R.Y., and X.Z. are the main designers and executors of the study and the manuscript. They have accessed and verified the data and share the first authorship. K.Z. and S. Kevin Z. conceive the original idea and provide supervision on the methodological design and content development of the paper. They also review and revise the manuscript and make the final decision on submission. W.W., C.L., Z.J., H.Z., J.L., M.L., and W.C. provide expert medical guidance and contributed the clinical evaluation results from human physicians. Z.J. participates in the writing of the introduction section of the paper and provides some revision suggestions for the results. All authors have read and approved the final version of the manuscript.

Competing interests

The authors declare no competing interests.

Inclusion and ethics statement

Not relevant.

References

[1] Chang, Y. *et al.* A survey on evaluation of large language models. *ACM transactions on intelligent systems and technology* **15**, 1–45 (2024).

[2] Gomez-Cabello, C. A. *et al.* Artificial-intelligence-based clinical decision support systems in primary care: A scoping review of current clinical implementations. *European Journal of Investigation in Health, Psychology and Education* **14**, 685–698 (2024).

[3] Delourme, S., Redjdal, A., Bouaud, J. & Seroussi, B. Measured performance and healthcare professional perception of large language models used as clinical decision support systems: A scoping review. *Stud. Health Technol. Inform* **316**, 841–845 (2024).

[4] Jin, Q., Dhingra, B., Liu, Z., Cohen, W. W. & Lu, X. Pubmedqa: A dataset for biomedical research question answering. *arXiv preprint arXiv:1909.06146* (2019).

[5] Jin, D. *et al.* What disease does this patient have? a large-scale open domain question answering dataset from medical exams. *Applied Sciences* **11**, 6421 (2021).

[6] Thirunavukarasu, A. J. *et al.* Large language models in medicine. *Nature medicine* **29**, 1930–1940 (2023).

[7] Singhal, K. *et al.* Toward expert-level medical question answering with large language models. *Nature Medicine* 1–8 (2025).

[8] Chen, Z. *et al.* Meditron-70b: Scaling medical pretraining for large language models. *arXiv preprint arXiv:2311.16079* (2023).

[9] Hager, P. *et al.* Evaluation and mitigation of the limitations of large language models in clinical decision-making. *Nature medicine* **30**, 2613–2622 (2024).

[10] Gaber, F. *et al.* Evaluating large language model workflows in clinical decision support for triage and referral and diagnosis. *npj Digital Medicine* **8**, 1–14 (2025).

[11] Bedi, S. *et al.* A systematic review of testing and evaluation of healthcare applications of large language models (llms). *medRxiv* 2024–04 (2024).

[12] Chen, J. *et al.* Huatuogpt-o1, towards medical complex reasoning with llms. *arXiv preprint arXiv:2412.18925* (2024).

[13] Zhao, J., Guo, Q., Liang, J., Li, Z. & Xiao, Y. Effective in-context learning for named entity recognition. In *2024 IEEE International Conference on Bioinformatics and Biomedicine (BIBM)*, 1376–1382 (IEEE, 2024).

[14] Sahoo, P. *et al.* A systematic survey of prompt engineering in large language models: Techniques and applications. *arXiv preprint arXiv:2402.07927* (2024).

[15] Wu, S., Koo, M., Scalzo, F. & Kurtz, I. Automedprompt: A new framework for optimizing llm medical prompts using textual gradients. *arXiv preprint arXiv:2502.15944* (2025).

[16] Savage, T., Nayak, A., Gallo, R., Rangan, E. & Chen, J. H. Diagnostic reasoning prompts reveal the potential for large language model interpretability in medicine. npj digital medicine, 7 (1), 20. *URL https://www. nature. com/articles/s41746-024-01010-1* (2024).

[17] Guo, G. *et al.* Structured outputs enable general-purpose llms to be medical experts. *arXiv preprint arXiv:2503.03194* (2025).

[18] Madaan, A. *et al.* Self-refine: Iterative refinement with self-feedback. *Advances in Neural Information Processing Systems* **36**, 46534–46594 (2023).

[19] Thomas, L. H. *et al.* Guidelines in professions allied to medicine. *Cochrane Database of Systematic Reviews* **2010** (1996).

[20] Custers, E. J. Thirty years of illness scripts: theoretical origins and practical applications. *Medical teacher* **37**, 457–462 (2015).

[21] Konstantinides, S. V. *et al.* 2019 esc guidelines for the diagnosis and management of acute pulmonary embolism developed in collaboration with the european respiratory society (ers) the task force for the diagnosis and management of acute pulmonary embolism of the european society of cardiology (esc). *European heart journal* **41**, 543–603 (2020).

[22] Metlay, J. P. *et al.* Diagnosis and treatment of adults with community-acquired pneumonia. an official clinical practice guideline of the american thoracic society and infectious diseases society of america. *American journal of respiratory and critical care medicine* **200**, e45–e67 (2019).

[23] Torres, A. *et al.* International ers/esicm/escmid/alat guidelines for the management of hospital-acquired pneumonia and ventilator-associated pneumonia: Guidelines for the management of hospital-acquired pneumonia (hap)/ventilator-associated pneumonia (vap) of the european respiratory society (ers), european society of intensive care medicine (esicm), european society of clinical microbiology and infectious diseases (escmid) and asociación latinoamericana del tórax (alat). *European Respiratory Journal* **50** (2017).

[24] Asteggiano, R., Bueno, H., Caforio, A., Carerj, S. & Ceconi, C. 2015 esc guidelines for the diagnosis and management of pericardial diseases–web addenda. *Eur Heart J* (2015).

[25] Leppäniemi, A. *et al.* 2019 wses guidelines for the management of severe acute pancreatitis. *World journal of emergency surgery* **14**, 1–20 (2019).

[26] Sartelli, M. *et al.* 2020 update of the wses guidelines for the management of acute colonic diverticulitis in the emergency setting. *World Journal of Emergency Surgery* **15**, 1–18 (2020).

[27] Pisano, M. *et al.* 2020 world society of emergency surgery updated guidelines for the diagnosis and treatment of acute calculus cholecystitis. *World journal of emergency surgery* **15**, 1–26 (2020).

[28] Di Saverio, S. *et al.* Wses jerusalem guidelines for diagnosis and treatment of acute appendicitis. *World Journal of Emergency Surgery* **11**, 1–25 (2016).

[29] Di Saverio, S. *et al.* Diagnosis and treatment of acute appendicitis: 2020 update of the wses jerusalem guidelines. *World journal of emergency surgery* **15**, 1–42 (2020).

[30] Appendicitis - Symptoms and causes. URL `https://www.mayoclinic.org/diseases-conditions/appendicitis/symptoms-causes/syc-20369543`.

[31] Cholecystitis - Symptoms and causes. URL `https://www.mayoclinic.org/diseases-conditions/cholecystitis/symptoms-causes/syc-20364867`.

[32] Diverticulitis - Symptoms and causes. URL `https://www.mayoclinic.org/diseases-conditions/diverticulitis/symptoms-causes/syc-20371758`.

[33] Pancreatitis - Symptoms and causes. URL `https://www.mayoclinic.org/diseases-conditions/pancreatitis/symptoms-causes/syc-20360227`.

[34] Pericarditis - Symptoms and causes. URL `https://www.mayoclinic.org/diseases-conditions/pericarditis/symptoms-causes/syc-20352510`.

[35] Pneumonia - Symptoms and causes. URL `https://www.mayoclinic.org/diseases-conditions/pneumonia/symptoms-causes/syc-20354204`.

[36] Pulmonary embolism - Symptoms and causes. URL `https://www.mayoclinic.org/diseases-conditions/pulmonary-embolism/symptoms-causes/syc-20354647`.

[37] Meta, A. Introducing llama 3.1: Our most capable models to date, 2024. *URL https://ai. meta. com/blog/meta-llama-3-1/. New models including flagship 405B parameter model, along with upgraded 8B and 70B models featuring 128K context length and multilingual capabilities* (2024).

[38] Guo, D. *et al.* Deepseek-r1: Incentivizing reasoning capability in llms via reinforcement learning. *arXiv preprint arXiv:2501.12948* (2025).

[39] Goldberger, A. L. *et al.* Physiobank, physiotoolkit, and physionet: components of a new research resource for complex physiologic signals. *circulation* **101**, e215–e220 (2000).

[40] Chen, X. *et al.* Enhancing diagnostic capability with multi-agents conversational large language models. *NPJ digital medicine* **8**, 159 (2025).

[41] Bedi, S., Jain, S. S. & Shah, N. H. Evaluating the clinical benefits of llms. *Nature Medicine* **30**, 2409–2410 (2024).

[42] Kwon, T. *et al.* Large language models are clinical reasoners: Reasoning-aware diagnosis framework with prompt-generated rationales. In *Proceedings of the AAAI conference on artificial intelligence*, vol. 38, 18417–18425 (2024).

[43] Zhou, S. *et al.* Large language models for disease diagnosis: A scoping review. *arXiv preprint arXiv:2409.00097* (2024).

[44] Wei, J. *et al.* Chain-of-thought prompting elicits reasoning in large language models. *Advances in neural information processing systems* **35**, 24824–24837 (2022).

[45] Wang, L. *et al.* Prompt engineering in consistency and reliability with the evidence-based guideline for llms. *NPJ digital medicine* **7**, 41 (2024).

[46] Yao, S. *et al.* Tree of thoughts: Deliberate problem solving with large language models. *Advances in neural information processing systems* **36**, 11809–11822 (2023).

[47] Deka, P., Jurek-Loughrey, A. & P, D. Evidence extraction to validate medical claims in fake news detection. In *International Conference on Health Information Science*, 3–15 (Springer, 2022).

Supplementary Information

S1 Dataset Composition

Supplementary Table 1: Dataset Composition.

	Appendicitis	Cholecystitis	Diverticulitis	Pancreatitis	Pericarditis	Pneumonia	Pulmonary embolism
All cases	957	648	257	538	114	1024	852
Sampling set	240	221	134	208	57	223	231
Learning set	90	90	90	90	23	90	90
Evaluation set	717	427	123	330	57	801	621

S2 Performance of Zero Knowledge across Various Diseases

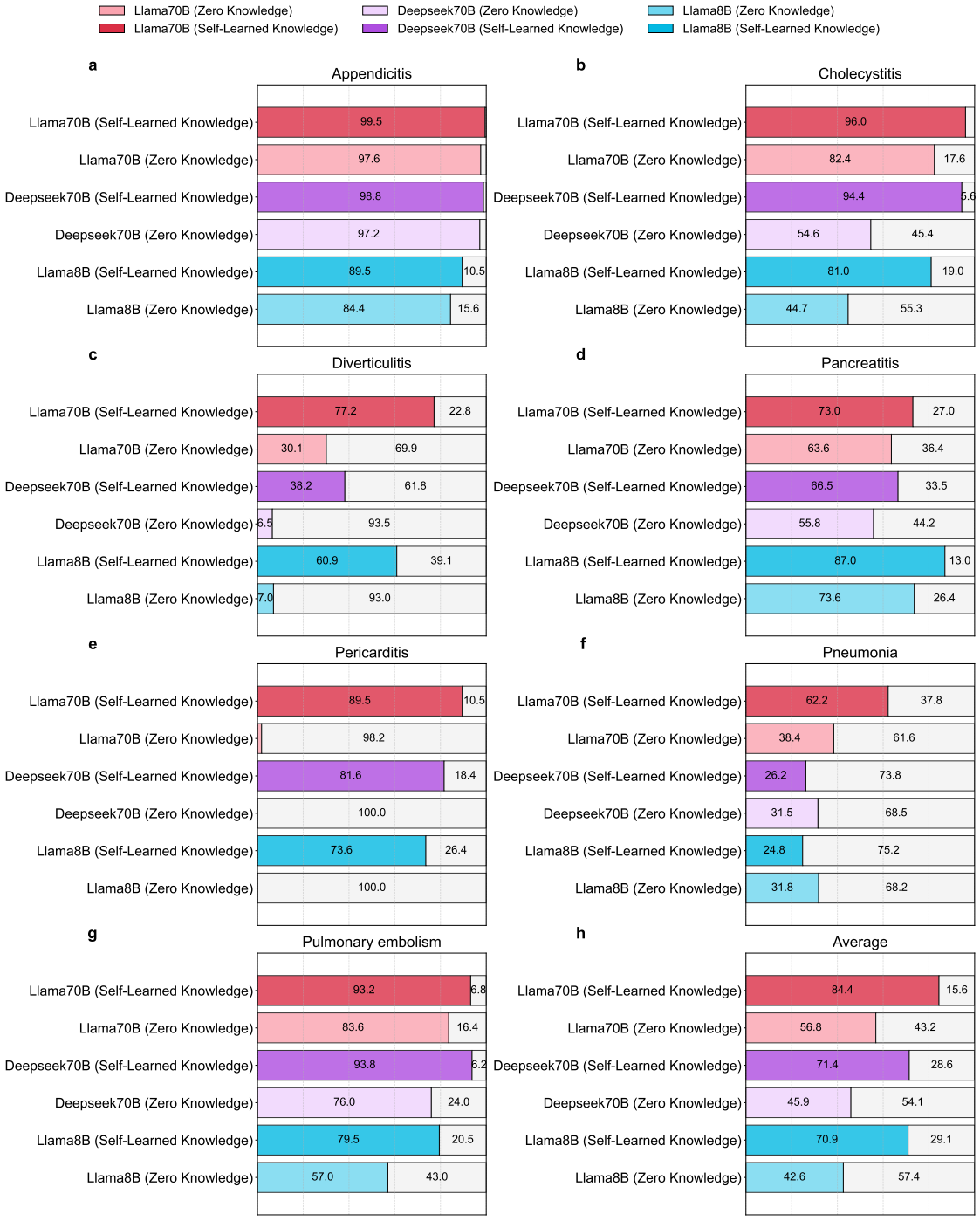

Supplementary Figure 1: **The MACD framework outperforms the zero-knowledge baseline in diagnostic accuracy.** LLMs performed diagnoses based solely on its internal parameters without any knowledge or reference, to represent the model's intrinsic diagnostic capability.

S3 Diagnostic Accuracy Comparison of Different Methods Across Various Diseases

Supplementary Table 2: Performance Comparison of Different Methods Across Various Diseases

Base Model	Methods	Appendicitis	Cholecystitis	Diverticulitis	Pancreatitis	Pericarditis	Pneumonia	Pulmonary embolism	Average
Llama3.1 -8B	COT	0.858	0.536	0.236	0.609	0.158	0.217	0.620	0.462
	Few Shot	**0.914**	0.419	0.195	0.727	0.018	0.126	0.691	0.441
	Ours	0.895	**0.810**	**0.609**	**0.870**	**0.736**	**0.248**	**0.795**	**0.709**
DeepSeek -70B	COT	0.939	0.621	0.244	0.542	0.105	**0.433**	0.717	0.514
	Few Shot	0.950	0.344	0.146	0.564	0.035	0.286	0.818	0.449
	Ours	**0.988**	**0.944**	**0.382**	**0.665**	**0.816**	0.262	**0.938**	**0.714**
Llama3.1 -70B	COT	0.964	0.707	0.447	0.582	0.123	0.456	0.773	0.579
	Few Shot	0.972	0.707	0.439	0.642	0.123	0.411	0.870	0.595
	Ours	**0.995**	**0.960**	**0.772**	**0.730**	**0.895**	**0.622**	**0.932**	**0.844**

S4 Comparison with Guideline Knowledge in Various Disease

Supplementary Table 3: Comparison with Different Guideline Knowledge in Various Disease

Model	**Type**	**Appendicitis**	**Cholecystitis**	**Diverticulitis**	**Pancreatitis**	**Pericarditis**	**Pneumonia**	**Pulmonary embolism**	**Average**
Llama 8B	Self-Learned Knowledge	0.895	**0.81**	0.609	0.87	**0.736**	**0.248**	0.795	**0.709**
	Guideline	**0.915**	0.4918	0.5366	**0.888**	0.5965	0.0637	**0.813**	0.615
	Mayo Clinic Guideline	0.728	0.799	**0.707**	0.544	0.474	0.146	0.784	0.597
	Professional Guideline								
Deepseek 70B	Self-Learned Knowledge	**0.988**	**0.944**	**0.382**	**0.665**	0.816	**0.262**	0.938	**0.714**
	Guideline	0.978	0.656	0.293	0.597	**0.825**	0.059	0.805	0.602
	Mayo Clinic Guideline	0.981	0.827	0.373	0.658	0.614	0.141	**0.973**	0.652
	Professional Guideline								
Llama 70B	Self-Learned Knowledge	**0.995**	**0.960**	**0.772**	**0.730**	**0.895**	**0.622**	**0.932**	**0.844**
	Guideline	0.990	0.902	0.675	0.727	0.684	0.398	0.886	0.752
	Mayo Clinic Guideline	0.757	0.375	0.675	0.611	0.649	0.437	0.840	0.621
	Professional Guideline								

S5 Self-Learned Knowledge of Different Models

S5.1 Self-Learned Knowledge of Llama-3.1-8B

Supplementary Table 4: Self-Learned Knowledge of Llama-3.1-8B

Pathology name	Type	Self-Learned Knowledge
Appendicitis	general	Initial periumbilical abdominal pain that localizes to the Right Lower Quadrant (RLQ) Some individuals experience general discomfort, fatigue, or lack of interest in food before experiencing more severe symptoms. Change in Stool Consistency. Nausea/Vomiting. Imaging findings of a dilated appendix Localized RLQ tenderness with rebound and involuntary guarding
	rare	Recurrent episodes of RLQ abdominal pain over an extended period Cases might also feature secondary infections or co-morbidities affecting overall patient health Blockage of the appendix can lead to its dilation and subsequent rupture Pain migration patterns vary among individuals, sometimes beginning centrally before moving to the RLQ. Certain cases involve retrocecal positioning, increasing the likelihood of perforation
Cholecystitis	general	Gallbladder wall appearance is 'indistinct and hazy' suggesting chronic inflammation No evidence of acute cholecystitis complications such as perforation, gangrene, or abscess formation Right upper quadrant (RUQ) and epigastric pain Presence of gallstones

Supplementary Table 4 – continued from previous page

Pathology name	Type	Self-Learned Knowledge
		Normal enhancement pattern of the liver and absence of intrahepatic biliary obstruction suggest that this condition is not related to obstructive jaundice.
Cholecystitis	rare	Circumferential wall edema up to 14mm Questionable focal wall interruption at the gallbladder fundus Adenomyomatosis (comet tail artifacts along the gallbladder wall) Presence of multiple gallstones (> 7) Presence of a small subhepatic/pericholecystic fluid collection Heterogeneous appearance and increased vascularity of the gallbladder wall
Diverticulitis	general	Imaging studies showing multiple diverticula in the distal thickened sigmoid colon Increased white blood cell count indicative of systemic inflammatory response syndrome. Presence of significant stranding around the sigmoid colon
	rare	Thickening of the sigmoid colon wall ($> 50\%$) Extraluminal air without organized collection, suggesting recent perforation Partial or complete blockage of the intestines by swollen segments, causing severe vomiting, abdominal tenderness, and cessation of gas passage. Loss of fat plane between the left ovary and the colon
Pancreatitis	general	Elevated serum lipase level (> 3 times the upper limit of normal) Severe epigastric pain radiating to back, often worse after eating. Presence of gallstone in the distal Common Bile Duct (CBD) Recent increased consumption of alcohol Markedly increased serum amylase/lipase levels indicative of pancreatic damage/enzyme leakage into bloodstream.

Supplementary Table 4 – continued from previous page

Pathology name	Type	Self-Learned Knowledge
	rare	Elevated lipase level Change in stool pattern from tan and solid to dark and loose Presence of diffuse dilation of the common bile duct with numerous filling defects on ERCP imaging
Pericarditis	general	Unilateral chest pain worsening with deep breathing and exertion Electrocardiographic Changes: Specific electrocardiogram patterns like low voltage QRS complexes (< 5mm), diffuse ST elevation without reciprocal changes, or PR interval prolongation. A distinctive friction rub heard over the precordium during auscultation. Elevated inflammatory markers (CRP > 10 mg/L) Mild tortuosity of the thoracic aorta Enlarged cardiac silhouette
	rare	Presence of pulsus paradoxus (> 10 mmHg) Normal echocardiogram showing no evidence of cardiac tamponade or ventricular dysfunction Positive family history of autoimmune diseases Mild metabolic acidosis and elevated white blood cell count suggesting inflammation Resolution of symptoms after drainage of the pericardial fluid Recent history of trauma (bike accident)

Supplementary Table 4 – continued from previous page

Pathology name	Type	Self-Learned Knowledge
Pneumonia	general	Respiratory Failure: Characterized by difficulty breathing, low oxygen saturation, and increased work of breathing, typically developing progressively. Fever: Temperature exceeding 38°C is noted in most cases, often with associated chills. Radiographic evidence of consolidation: Lobar or segmental consolidation visible on imaging. Physical examination findings: Coarse breath sounds, absent or diminished breath sounds, and localized crackles are detected, especially over the site of consolidation. Increased White Blood Cell Count: A hallmark sign of infection, often exceeding 12000 cells/microL with neutrophilic predominance. Altered Mental Status: Suggestive of systemic infection affecting brain function, particularly in older or severely ill patients. Productive cough: Cough producing purulent sputum.
	rare	Presence of Infection Markers: Such as elevated CRP and procalcitonin, indicative of ongoing bacterial infection rather than thrombotic inflammation. Patchy ill-defined opacity in the right lung base: Typically represents infection-related inflammation. Mild leukopenia: Some patients, especially immunocompromised, showed a decrease in total white blood cell count. Severe Hypoxemia: Extremely low oxygen saturation levels in the blood, necessitating urgent treatment. Severe Bronchospasm: Can accompany pneumonia in patients with underlying reactive airway disease. Presence of leukocytes in urine: Reflects systemic inflammatory response. Patchy infiltration: Ground-glass patches and multifocal consolidation are visible on CT scans, suggestive of infectious.

Supplementary Table 4 – continued from previous page

Pathology name	Type	Self-Learned Knowledge
Pulmonary Embolism	general	Sudden onset of shortness of breath Risk Factors: History of recent surgery, immobility, and previous trauma to the hips. Absence of signs of right heart strain on echocardiogram. Recent history of deep vein thrombosis (DVT). Underlying Condition: Presence of mixed connective tissue disease. Elevated D-Dimer Levels: Extremely high d-dimer levels exceeding expected ranges. Markedly low blood pressure requiring vasopressor support.
	rare	Markedly low blood pressure requiring vasopressor support. Low molecular weight heparin therapy discontinued before symptom onset. Low Platelet Count: Platelet count significantly below normal range. Simple renal cysts Echocardiographic evidence of increased RV pressure leading to dilatation. Small Right Pleural Effusion: Presence of trace right pleural effusion. Reflux of contrast within the IVC and hepatic veins.

S5.2 Self-Learned Knowledge of Deepseek-R1-Distill-Llama-70B

Supplementary Table 5: Self-Learned Knowledge of Deepseek-R1-Distill-Llama-70B

Pathology name	Type	Self-Learned Knowledge
Appendicitis	general	Right lower quadrant abdominal pain
		Tenderness at McBurney's point
		Elevated white blood cell count (ranging from 9.9 to 27.5 K/uL)
		Appendiceal wall thickening and luminal distension observed on CT imaging
		Nausea and vomiting
		Periappendiceal fat stranding on imaging
		Enlarged appendix (size varying from 6mm to over 1 cm)
	rare	Presence of appendicoliths on imaging
		Free pelvic fluid without overt signs of perforation
		Abscess formation or fluid collections
		Reactive periappendiceal lymph nodes
		Reactive terminal ileitis
		Absence of free air ruling out perforation
Cholecystitis	general	Positive sonographic Murphy's sign
		Right upper quadrant (RUQ) pain, often severe and persistent
		Elevated white blood cell count (leukocytosis)
		Gallbladder wall thickening (greater than 4mm) with pericholecystic fluid
		Presence of gallstones on imaging
		Mild elevation of liver enzymes (ALT/AST)
	rare	Proteinuria without significant hematuria
		Significantly elevated liver enzymes (ALT/AST) in the presence of choledocholithiasis
		Pericholecystic fluid collection, sometimes indicating gallbladder perforation or evolving abscess
		Layering sludge in the gallbladder without visible gallstones, seen in acalculous cholecystitis

Supplementary Table 5 – continued from previous page

Pathology name	Type	Self-Learned Knowledge
		Rim sign on CT
		Bile duct dilation with documented stones
Diverticulitis	general	Left lower quadrant (LLQ) abdominal tenderness on physical examination
		CT scan revealing diverticula and potential complications.
		Elevated white blood cell count
		Absence of free air or diffuse peritoneal signs on initial imaging, suggesting contained inflammation rather than perforation
		Clinical presentation includig abdominal pain, fever, constipation or diarrhea, and bloating
		CT imaging shows colonic wall thickening (commonly ¿4 mm) in the sigmoid colon, with pericolic fat stranding
	rare	Free air (pneumoperitoneum) on CT, indicating perforation
		Dark-colored stools or gastrointestinal (GI) bleeding
		Symptom improvement with antibiotics followed by relapse
		Extensive diverticulosis of the colon observed on CT, without active inflammation
		Widespread activation of immune cells throughout the body, potentially leading to shock, organ failure, or sepsis if left untreated.
		Extraluminal gas localized to the left lower quadrant
Pancreatitis	general	Elevated Amylase/Lipase $>$ 3 times the upper limit of normal
		Severe epigastric abdominal pain radiating to the back, often worsened by eating
		Persistent nausea and vomiting, often leading to dehydration
		Leukocytosis (elevated white blood cell count)
		Abdominal tenderness upon physical examination, but no rebound tenderness unless complicated by necrosis or infection
		Peripancreatic fluid collections and fat stranding with necrosis on CT

Supplementary Table 5 – continued from previous page

Pathology name	Type	Self-Learned Knowledge
Pancreatitis	rare	Severe nausea and vomiting leading to profound dehydration and electrolyte imbalances Biliary dilation or sludge without evidence of gallstone obstruction, suggesting biliary pancreatitis Peripancreatic fat necrosis confirmed by imaging, often with pancreatic parenchymal changes Unintentional weight loss (e.g., 30 lbs over three weeks) due to prolonged illness or exocrine insufficiency Leukoysis (High WBC Count) History of gallstone-related symptoms without acute cholecystitis features, but with signs of biliary pancreatitis
Pericarditis	general	Positional chest pain improving with sitting up and leaning forward Elevated inflammatory markers (e.g., CRP, ESR, WBC) Electrocardiogram showin ST elevations or prolonged PR intervals. Evidence of pericardial effusion on imaging studies (echocardiogram, CT, or radiography) Positional chest pain improving when sitting up and leaning forward Pericardial friction rub upon auscultation.
	rare	Signs of cardiac tamponade (distended neck veins, hypotension). High ESR with marked leukocyrosis (e.g., Neutrophils $\geq 75\%$) Radiographic evidence of water-bottle-shaped heart

Supplementary Table 5 – continued from previous page

Pathology name	Type	Self-Learned Knowledge
Pneumonia	general	Productive cough, often yellow, green, or blood-streaked sputum Low-grade to moderate fever (e.g., ¿100.4°F), commonly accompanied by chills and malaise Shortness of breath that is progressive, typically gradual onset Elevated white blood cell count with neutrophil predominance (neutrophilia), supporting infectious etiology Ground-glass opacities or lobar/segmental consolidations on chest imaging (X-ray or CT) Crackles (rales) or bronchial breath sounds heard on auscultation
	rare	Extensive lung consolidation involving multiple lobes, sometimes progressing to acute respiratory distress syndrome (ARDS) Hypoxemia unresponsive to oxygen therapy, indicating severe pulmonary involvement Weight loss, poor appetite, and night sweats, especially with chronic infections like tuberculosis or fungal pneumonia Bibasilar atelectasis visible on imaging, secondary to obstruction or infection Pleuritic chest pain that worsens with coughing or deep inspiration but does not improve with positional changes
Pulmonary Embolism	general	Filling defects in pulmonary arteries on CT angiography (e.g., main, segmental, or subsegmental branches) Tachycardia (rapid heart rate), typically defined as > 100 bpm Elevated D-dimer levels Hypoxia (low oxygen saturation, e.g., $SpO_2 < 90\%$) Signs of right ventricular strain on echocardiography Direct visualization of thrombi via CT pulmonary anglography. Sudden onset of dyspnea

Supplementary Table 5 – continued from previous page

Pathology name	**Type**	**Self-Learned Knowledge**
Pulmonary Embolism	rare	Wedge-shaped opacity consistent with pulmonary infarct Extremely elevated D-dimer levels (> 5000 ng/mL) Electrocardiogram abnormalities (e.g., ST segment depression, T wave inversion) Bilateral saddle emboli causing extensive occlusion Pro-BNP elevation (e.g., 1147 ng/mL) Presentation with cough, fever, and tachypnea Elevated Troponin and BNP levels indicating cardiac strain

S5.3 Self-Learned Knowledge of Llama-3.1-70B

Supplementary Table 6: Self-Learned Knowledge of Llama-3.1-70B

Pathology name	Type	Self-Learned Knowledge
Appendicitis	general	Abdominal pain localized to the right lower quadrant
		Elevated white blood cell count
		Presence of nausea and vomiting
		Presence of periappendiceal fat stranding
		Imaging findings of a dilated appendix
		Tenderness to palpation over the right lower quadrant
		Clinical presentation of nausea, vomiting, and fever
	rare	Presence of an appendicolith on imaging
		Trace periappendical stranding
		Non-filling of the appendix with mucosa hyperenhancement and dilatation of the appendiceal tip
		Migration of abdominal pain from the peri-umblical area to the right lower quadrant
		Free fluid tracking along the right paracolic gutter on computed tomography scan
		Fluid-filled and dilated appendix measuring up to 13 mm in diameter
		Dilation of the appendiceal tip, walls of the proximal and mid appendix are indistinct with surrounding fat standing, and adjacent cecal tip thickening
Cholecystitis	general	Right upper quadrant abdominal pain and tenderness
		Presence of multiple risk factors such as previous episodes of tumor flare-ups, recent changes in diabetic regimen leading to hypoglycemia, and use of Sorafenib therapy increasing the risk of thromboembolic events and subsequent development of ascending cholangitis
		Positive Sonographic Murphy's sign
		Imaging findings of dilated common bile ducts and choledocholithiasis on ultrasound abdomen
		Elevated white blood cell count

Supplementary Table 6 – continued from previous page

Pathology name	Type	Self-Learned Knowledge
Cholecystitis		Fever > 38°C (100.4°F)
		Elevated Liver enzymes (ALT, AST)
	rare	Perforation of the gallbladder with abscess formation
		Ischemic Gallbladder Necrosis due to Arterial Occlusion secondary to Pseudoaneurysms
		Ascending Cholangitis secondary to Choledochoolithiasis
		Presence of sludge within the gallbladder
		Gallbladder wall edema and minimal thickening ($< 3mm$)
		Absence of choelithiasis does not rule out acute cholecystitis
Diverticulitis	general	Surrounding fat stranding
		Leukocytosis (Elevated White Blood Cell Count)
		Presence of colonic diverticulosis on imaging studies
		Fever
		Thickening of the sigmoid colon
	rare	Contained perforation indicated by extraluminal air
		Small foci of extraluminal air adjacent to the sigmoid colon
		Notable involvement of the sigmoid mesocolon with surrounding fat stranding
		Micro-abscess formation
		Phlegmonous fluid collection interposed between the sigmoid colon and bladder
		Pneumoperitoneum due to perforation of diverticula
Pancreatitis	general	Elevated serum lipase level (> 3 times upper limit of normal)
		Nausea and vomiting
		Imaging findings suggestive of pancreatitis (enlargement, necrosis, or inflammation)
		Severe epigastric pain radiating to back, often worse after eating.
		Elevated serum amylase level
		Elevated white blood cell count indicating infection/inflammation.

Supplementary Table 6 – continued from previous page

Pathology name	Type	Self-Learned Knowledge
Pancreatitis		Imaging evidence such as CT scan showing pancreatic inflammation/enlargement
	rare	History of recent heavy ethanol consumption Imaging showing a pancreatic mass with surrounding inflammation and necrosis Worsening symptoms despite previous treatment Presence of gallstones and a dilated common bile duct on ultrasound Splenic vein thrombosis Post-endoscopic retrograde cholangiopancreatography (ERCP)-induced pancreatitis indicated by recent ERCP procedure Elevated liver enzymes indicative of associated liver involvement
Pericarditis	general	Pleuritic chest pain that worsens with deep breathing Elevated white blood cell count Pericardial friction rub upon auscultation. Normal cardiac biomarkers (e.g., Troponin-T < 0.01 ng/mL) Elevated inflammatory markers (such as CRP or ESR) Widened mediastinum on portable chest radiograph
	rare	Positional variation in chest pain (improvement with leaning forward) Uremic pericarditis due to end-stage renal disease (ESRD) Low-grade fever (< 101°F) Bibasilar linear opacities consistent with discoid atelectasis and mild bronchial wall thickening on imaging studies Presence of pericardial friction rub may be absent early in disease course Radiation-free chest pain exacerbated by deep breathing and movement

Supplementary Table 6 – continued from previous page

Pathology name	Type	Self-Learned Knowledge
		Malignant pericarditis due to metastatic disease from non-Hodgkin's lymphoma (NHL)
Pneumonia	general	Clinical presentation consistent with respiratory infection (fever, cough, productive sputum). Elevated white blood cell count Radiographic evidence of new infiltrate(s), lobar or segmental pattern Laboratory confirmation via Gram stain/culture of blood/sputum/tracheal aspirates or urinary antigen testing positive for Legionela pneumophilia or Streptococcus pneumoniae serotype Patient's history of possible aspiration event with oral secretions. Ground glass opacity in the right lower and middle lobe on CT scan indicating alveolar damage.
	rare	Recent history of dental procedure which may be considered as risk factor for aspiration pneumonia Underlying condition of chronic lymphocytic leukemia (CLL) making patient susceptible to infections. Bronchiectasis in the right lower lobe with peribronchial wall thickening. Presence of risk factors for aspiration including history of recurrent aspirations, seizures, and recent enteral feeding tube placement. Delirium secondary to pneumonia
Pulmonary Embolism	general	Sudden onset of dyspnea Presence of risk factors such as recent surgery, immobility, and malignancy Imaging findings of filling defects in the pulmonary arteries on CT scan Elevated D-dimer level ($>$ 1000 ng/ml)

Supplementary Table 6 – continued from previous page

Pathology name	Type	Self-Learned Knowledge
		Pleuritic chest pain
Pulmonary Embolism	rare	Extensive bilateral pulmonary emboli including a saddle embolus at the bifurcation of the main pulmonary artery History of breast cancer with current radiation therapy and recent discontinuation of anticoagulation therapy Heterozygosity for the prothrombin gene mutation indicating inherited thrombophilia Wedge-shaped, peripheral-based consolidation consistent with pulmonary infarct Near occlusive acute thrombus within the right main pulmonary artery with extension into the lobar, segmental and subsegmental branches of the right lung Central filling defects in the right main, right middle, interlobar, and posterior basal segmental pulmonary arteries consistent with acute PE

S6 Ablation Study of Concepts Importance

S6.1 Ablation Study on Concepts Importance of Llama-3.1-8B

Supplementary Table 7: Ablation Study on Concepts Importance of Llama-3.1-8B

		Appendicitis	Cholecystitis	Diverticulitis	Pancreatitis	Pericarditis	Pneumonia	Pulmonary embolism
Llama3.1-8B	Concepts-1	0.493	0.748	0.712	0.818	0.649	0.166	0.790
	Concepts-2	0.602	0.892	0.728	0.836	0.667	0.165	0.777
	Concepts-3	0.587	0.890	0.728	0.814	0.605	0.172	0.795
	Concepts-4	0.578	0.861	0.696	0.809	0.640	0.176	0.762
	Concepts-5	0.595	0.846	0.708	0.816	0.605	0.187	0.785
	Concepts-6	0.494	0.872	0.712	0.827	0.816	0.179	0.791
	Concepts-7	0.572	0.824	0.704	0.838	0.675	0.164	0.783
	Concepts-8	0.568	0.869	0.700	0.831	0.667	0.178	0.788
	Concepts-9	0.581	0.896	0.704	0.833	0.658	0.179	0.789
	Concepts-10	0.599	0.881	0.720	0.822	0.754	0.181	0.785
	Concepts-11	0.564	0.884	0.708	0.825	0.570	0.184	0.786
	Concepts-12	0.681	0.880	0.728	0.825	0.632	0.179	0.797
	Concepts-13	0.588	0.875	0.708	0.836	0.675	0.189	0.789
	Concepts-14	None	0.871	0.716	0.823	0.667	0.193	0.785
	Full Prompt	0.597	0.886	**0.708**	0.825	0.684	0.196	0.794
	Remove Concepts	**0.897**	0.890	0.700	**0.877**	**0.842**	**0.286**	**0.830**

S6.2 Ablation Study on Concepts Importance of Deepseek-R1-Distill-Llama-70B

Supplementary Table 8: Ablation Study on Concepts Importance of Deepseek-R1-Distill-Llama-70B

		Appendicitis	Cholecystitis	Diverticulitis	Pancreatitis	Pericarditis	Pneumonia	Pulmonary embolism
Deepseek-R1-Distill-Llama-70B	Concepts-1	0.991	0.974	0.498	0.533	0.781	0.201	0.892
	Concepts-2	0.990	0.958	0.553	0.608	0.789	0.234	0.905
	Concepts-3	0.989	0.955	0.541	0.667	0.868	0.245	0.898
	Concepts-4	0.989	0.954	0.576	0.660	0.825	0.198	0.899
	Concepts-5	0.990	0.971	0.572	0.647	0.825	0.210	0.906
	Concepts-6	0.989	0.963	0.564	0.652	0.781	0.152	0.903
	Concepts-7	0.983	0.971	0.529	0.665	0.807	0.266	0.913
	Concepts-8	0.991	0.958	0.545	0.665	0.807	0.238	0.906
	Concepts-9	0.990	0.961	0.556	0.665	0.816	0.236	0.906
	Concepts-10	0.989	0.964	0.564	0.664	0.851	0.193	0.907
	Concepts-11	0.991	0.961	0.564	0.651	0.851	0.275	0.906
	Concepts-12	0.990	0.961	0.549	0.665	0.825	0.268	0.912
	Concepts-13	0.989	0.968	0.533	0.688	0.851	0.236	0.915
	Concepts-14	0.989	None	0.560	0.664	0.887	0.210	0.904
	Full Prompt	0.987	0.966	0.568	0.660	0.833	0.219	0.914
	Remove Concepts	**0.987**	**0.968**	**0.607**	**0.693**	**0.842**	**0.269**	**0.953**

S6.3 Ablation Study on Concepts Importance of Llama-3.1-70B-Instruct

Supplementary Table 9: Ablation study of concepts importance

		Appendicitis	Cholecystitis	Diverticulitis	Pancreatitis	Pericarditis	Pneumonia	Pulmonary embolism
Llama3.1-70B	Concepts-1	0.994	0.981	0.856	0.643	0.912	0.714	0.915
	Concepts-2	0.995	0.986	0.852	0.725	0.974	0.716	0.921
	Concepts-3	0.995	0.988	0.837	0.727	0.956	0.701	0.919
	Concepts-4	0.996	0.989	0.821	0.699	0.921	0.721	0.918
	Concepts-5	0.993	0.991	0.837	0.719	0.903	0.742	0.927
	Concepts-6	0.993	0.991	0.825	0.721	0.903	0.699	0.927
	Concepts-7	0.996	0.983	0.833	0.723	0.939	0.654	0.917
	Concepts-8	0.992	0.989	0.825	0.712	0.929	0.739	0.915
	Concepts-9	0.996	0.991	0.837	0.727	0.929	0.719	0.920
	Concepts-10	0.995	0.992	0.829	0.721	0.939	0.740	0.914
	Concepts-11	0.993	0.989	0.825	0.691	0.921	0.725	0.906
	Concepts-12	0.991	0.988	0.837	0.734	0.938	0.738	0.947
	Concepts-13	0.993	0.986	0.827	0.704	0.938	0.736	0.913
	Concepts-14	0.991	0.984	0.844	0.704	0.947	0.715	0.897
	Full Prompt	0.995	**0.989**	0.840	0.732	**0.965**	0.722	0.921
	Remove Concepts	**0.995**	0.986	**0.875**	**0.752**	0.938	**0.734**	**0.946**

S7 The Mayo Clinic Guideline

Supplementary Table 10: The Mayo Clinic Guideline

Pathology name	Content
Appendicitis	Appendicitis is an inflammation of the appendix. The appendix is a finger-shaped pouch that sticks out from the colon on the lower right side of the belly, also called the abdomen. Symptoms of appendicitis may include: - Sudden pain that begins on the right side of the lower belly. - Sudden pain that begins around the belly button and often shifts to the lower right belly. - Pain that worsens with coughing, walking or making other jarring movements. - Nausea and vomiting. - Loss of appetite. - Low-grade fever that may rise as the illness worsens. - Constipation or diarrhea. - Belly bloating. - Gas. Tests used to diagnose appendicitis include: Physical exam. A healthcare professional may apply gentle pressure on the painful area. When the pressure is suddenly released, appendicitis pain will often feel worse. This is because of inflammation of the lining of the abdominal cavity, called the peritoneum. A care professional also may look for abdominal stiffness and a tendency to flex the abdominal muscles in response to pressure over the inflamed appendix. This is called guarding. A care professional also may use a lubricated, gloved finger to examine the lower rectum. This is called a digital rectal exam. People of childbearing age may be given a pelvic exam to check for other problems that could be causing the pain. Blood test. This test checks for a high white blood cell count. A high white blood cell count may mean there's an infection.

Supplementary Table 10 – continued from previous page

Pathology name	Content
	Urine test. A urine test, also called a urinalysis, may be done. A urinalysis makes sure that a urinary tract infection or a kidney stone isn't causing the pain. Imaging tests. Imaging tests may help confirm appendicitis or find other causes for pain. These tests may include an abdominal X-ray, an abdominal ultrasound, a CT scan or an MRI.
Cholecystitis	Cholecystitis (ko-luh-sis-TIE-tis) is swelling and irritation, called inflammation, of the gallbladder. The gallbladder is a small, pear-shaped organ on the right side of the belly under the liver. The gallbladder holds fluid that digests food. This fluid is called bile. The gallbladder releases bile into the small intestine. Symptoms of cholecystitis may include: - Severe pain in the upper right or center belly area. - Pain that spreads to the right shoulder or back. - Tenderness over the belly area when it's touched. - Nausea. - Vomiting. - Fever. Tests and procedures used to diagnose cholecystitis include: Blood tests. Blood tests can look for signs of an infection or other gallbladder issues. Imaging tests that show your gallbladder. Abdominal ultrasound, endoscopic ultrasound, CT scan or magnetic resonance cholangiopancreatography can make pictures of your gallbladder and bile ducts. These pictures may show signs of cholecystitis or stones in the bile ducts and gallbladder. A scan that shows the movement of bile through the body. A hepatobiliary iminodiacetic acid (HIDA) scan tracks the making and flow of bile from the liver to the small intestine. A HIDA scan involves putting a radioactive dye into your body. The dye attaches to the cells that make bile. During the scan, the dye can be seen as it travels with the bile through the bile ducts. This can show any blockages.

Supplementary Table 10 – continued from previous page

Pathology name	Content
Diverticulitis	Diverticulitis is inflammation of irregular bulging pouches in the wall of the large intestine. A common symptom of diverticulitis is pain in the area below the chest called the abdomen. Most often, pain is in the lower left abdomen. Pain from diverticulitis is usually sudden and intense. Pain may be mild and gradually worsen, or the intensity of the pain may vary over time. Other signs and symptoms of diverticulitis may include: - Nausea. - Fever. - Tenderness in the abdomen when touched. - Changes in stool, including sudden diarrhea or constipation. During the physical exam, your healthcare professional will gently touch different parts of the abdomen to learn where you have pain or tenderness. An exam also may include a pelvic exam to test for disease of the female reproductive organs. Laboratory tests may be used to rule out other conditions and make a diagnosis: Blood tests for signs of infection and immune-system activity. Urine test. Stool test. Pregnancy test. Liver enzyme test to rule out liver disease. A computerized tomography (CT) scan can show inflamed diverticula, abscesses, fistulas or other complications.
Pancreatitis	Pancreatitis is inflammation of the pancreas. Inflammation is immune system activity that can cause swelling, pain, and changes in how an organ or tissues work. Symptoms of pancreatitis may vary. Acute pancreatitis symptoms may include: - Pain in the upper belly. - Pain in the upper belly that radiates to the back. - Tenderness when touching the belly. - Fever.

Supplementary Table 10 – continued from previous page

Pathology name	Content
Pancreatitis	- Rapid pulse. - Upset stomach. - Vomiting. Chronic pancreatitis signs and symptoms include: - Pain in the upper belly. - Belly pain that feels worse after eating. - Losing weight without trying. - Oily, smelly stools. Tests and procedures that may be used include the following. Blood tests can give clues about how the immune system, pancreas and related organs are working. Ultrasound images can show gallstones in the gallbladder or inflammation of the pancreas. Computerized tomography (CT) scan show gallstones and the extent of inflammation. Magnetic resonance imaging (MRI) to look for irregular tissues or structures in the gallbladder, pancreas and bile ducts. Endoscopic ultrasound is an ultrasound device on a small tube fed through the mouth and into the digestive system. It can show inflammation, gallstones, cancer, and blockages in the pancreatic duct or bile duct. Stool tests can measure levels of fat that could suggest your digestive system isn't absorbing nutrients as it should.
Pericarditis	Pericarditis is swelling and irritation of the thin, saclike tissue surrounding the heart. This tissue is called the pericardium. Pericarditis often causes sharp chest pain. The chest pain occurs when the irritated layers of the pericardium rub against each other. Most often, pericarditis pain is felt behind the breastbone or on the left side of the chest. The pain may: - Spread to the left shoulder and neck, or to both shoulders. - Get worse when coughing, lying down or taking a deep breath. - Get better when sitting up or leaning forward.

Supplementary Table 10 – continued from previous page

Pathology name	Content
Pericarditis	Other symptoms of pericarditis can include: - Cough. - Fatigue or general feeling of weakness or being sick. - Swelling of the legs or feet. - Low-grade fever. - Pounding or racing heartbeat, also called heart palpitations. - Shortness of breath when lying down. - Swelling of the belly, also called the abdomen. Tests to diagnose pericarditis or rule out conditions that may cause similar symptoms may include: Blood tests. Blood tests usually are done to check for signs of a heart attack, inflammation and infection. Electrocardiogram (ECG). An electrocardiogram is a quick and painless test that records the electrical signals in the heart. It can show how the heart is beating. Sticky patches called electrodes with wires attach to the chest and sometimes the arms or legs. The wires connect to a monitor, which prints or displays results. Chest X-ray. A chest X-ray can show changes in the size and shape of the heart. It can tell if the heart is enlarged. Echocardiogram. Sound waves create images of the moving heart. An echocardiogram shows how well the heart is pumping blood. It also can see any fluid buildup in the tissue surrounding the heart. The test can tell if the sac surrounding the heart affects the way the heart fills with blood or pumps blood. Cardiac computerized tomography (CT) scan. Cardiac CT scans use X-rays to create images of the heart and chest. The test can be used to look for heart thickening that may be a sign of constrictive pericarditis. Cardiac magnetic resonance imaging (MRI). This test uses magnetic fields and radio waves to create detailed images of the heart. A cardiac MRI scan can show thickening, inflammation or other changes in the thin tissue surrounding the heart.

Supplementary Table 10 – continued from previous page

Pathology name	Content
Pneumonia	Pneumonia is an infection that inflames the air sacs in one or both lungs. The air sacs may fill with fluid or pus (purulent material), causing cough with phlegm or pus, fever, chills, and difficulty breathing. A variety of organisms, including bacteria, viruses and fungi, can cause pneumonia. Signs and symptoms of pneumonia may include: - Chest pain when you breathe or cough - Confusion or changes in mental awareness (in adults age 65 and older) - Cough, which may produce phlegm - Fatigue - Fever, sweating and shaking chills - Lower than normal body temperature (in adults older than age 65 and people with weak immune systems) - Nausea, vomiting or diarrhea - Shortness of breath If pneumonia is suspected, your doctor may recommend the following tests: Blood tests. Blood tests are used to confirm an infection and to try to identify the type of organism causing the infection. However, precise identification isn't always possible. Chest X-ray. This helps your doctor diagnose pneumonia and determine the extent and location of the infection. However, it can't tell your doctor what kind of germ is causing the pneumonia. Pulse oximetry. This measures the oxygen level in your blood. Pneumonia can prevent your lungs from moving enough oxygen into your bloodstream. Sputum test. A sample of fluid from your lungs (sputum) is taken after a deep cough and analyzed to help pinpoint the cause of the infection. Your doctor might order additional tests if you're older than age 65, are in the hospital, or have serious symptoms or health conditions. These may include: CT scan. If your pneumonia isn't clearing as quickly as expected, your doctor may recommend a chest CT scan to obtain a more detailed image of your lungs. Pleural fluid culture. A fluid sample is taken by putting a needle between your ribs from the pleural area and analyzed to help determine the type of infection.

Supplementary Table 10 – continued from previous page

Pathology name	Content
pulmonary embolism	A pulmonary embolism is a blood clot that blocks and stops blood flow to an artery in the lung. In most cases, the blood clot starts in a deep vein in the leg and travels to the lung. Rarely, the clot forms in a vein in another part of the body. When a blood clot forms in one or more of the deep veins in the body, it's called a deep vein thrombosis (DVT). Common symptoms include: - Shortness of breath. This symptom usually appears suddenly. Trouble catching your breath happens even when resting and gets worse with physical activity. - Chest pain. You may feel like you're having a heart attack. The pain is often sharp and felt when you breathe in deeply. The pain can stop you from being able to take a deep breath. You also may feel it when you cough, bend or lean over. - Fainting. You may pass out if your heart rate or blood pressure drops suddenly. This is called syncope. Other symptoms that can occur with pulmonary embolism include: - A cough that may include bloody or blood-streaked mucus - Rapid or irregular heartbeat - Lightheadedness or dizziness - Excessive sweating - Fever - Leg pain or swelling, or both, usually in the back of the lower leg - Clammy or discolored skin, called cyanosis Blood tests. Your health care provider may order a blood test for the clot-dissolving substance D dimer. High levels may suggest an increased likelihood of blood clots, although many other factors can cause high D dimer levels. Chest X-ray. This noninvasive test shows images of your heart and lungs on film. Although X-rays can't diagnose a pulmonary embolism and may even appear fine when a pulmonary embolism exists, they can rule out other conditions with similar symptoms.

Supplementary Table 10 – continued from previous page

Pathology name	Content
pulmonary embolism	Ultrasound. A noninvasive test known as duplex ultrasonography, sometimes called a duplex scan or compression ultrasonography, uses sound waves to scan veins to check for deep vein blood clots. This test can look at veins in the thigh, knee and calf, and sometimes the arms. CT pulmonary angiography. CT scanning generates X-rays to produce cross-sectional images of your body. CT pulmonary angiography — also called a CT pulmonary embolism study — creates 3D images that can find changes such as a pulmonary embolism within the arteries in your lungs. Ventilation-perfusion (V/Q) scan. When there is a need to avoid radiation exposure or contrast from a CT scan due to a medical condition, a V/Q scan may be done. In this test, a small amount of a radioactive substance called a tracer is injected into a vein in your arm. The tracer maps blood flow, called perfusion, and compares it with the airflow to your lungs, called ventilation. This test can be used to see if blood clots are causing symptoms of pulmonary hypertension. Pulmonary angiogram. This test provides a clear picture of the blood flow in the arteries of your lungs. It's the most accurate way to diagnose a pulmonary embolism. But because it requires a high degree of skill to perform and has potentially serious risks, it's usually done when other tests fail to provide a definite diagnosis. MRI. MRI is a medical imaging technique that uses a magnetic field and computer-generated radio waves to create detailed images of the organs and tissues in your body. MRI is usually only done in those who are pregnant — to avoid radiation to the baby — and in people whose kidneys may be harmed by dyes used in other tests.

S8 Prompt Instruction for the Constraction of Professional Guideline

You are a medical AI assistant. Your task is to summarize the relevant diagnostic criteria for diseases from professional diagnostic guidelines.

I will provide you with diagnostic guidelines for appendicitis, cholecystitis, diverticulitis, and pancreatitis, and you will need to summarize the corresponding diagnostic criteria or features from these guidelines.

requirement:
1. These diagnostic criteria must be explicitly mentioned in the guidelines, which can be mentioned in the pictures or in the text section. Please do not include your knowledge.
2. The diagnostic criteria for summarizing require each disease to be output separately in the same format, which can include physical examination, blood examination, imaging examination, etc. If there is no diagnostic basis or diagnostic feature for any part of it, the corresponding content may not be output.
3. Require semantic conciseness, only outputting the most relevant content for diagnosis, without additional output.
4. You can adjust the order of the content appropriately, or add some related words or dots to list the diagnostic criteria or features, but you cannot output content that is not mentioned in the guide.

S9 The Professional Guideline

Supplementary Table 11: The Professional Guideline

Pathology name	Content
Appendicitis	Clinical Features & Physical Examination: - Diagnosis can be challenging; individual clinical variables have low diagnostic value. - Migratory abdominal pain and signs of peritonitis are important distinguishing features. Laboratory Tests: - Inflammatory markers (e.g., white blood cell count, CRP) are important distinguishing features. - If two or more inflammatory markers are normal, appendicitis is unlikely; if two or more are elevated, appendicitis is very likely. - Pediatric patients: White blood cell count (WBC), absolute neutrophil count (ANC), C-reactive protein (CRP), and urinalysis should be routinely checked. CRP $\geq 10mg/L$ and WBC count $\geq 16,000/mL$ are strong predictive factors for appendicitis in children. Clinical Scoring Systems: - An Alvarado score < 5 is sufficiently sensitive to exclude acute appendicitis. - The AIR score and AAS score are currently the best-performing clinical prediction scores in adults with suspected acute appendicitis. An AIR score < 4 (low probability) has high sensitivity (0.96) for appendicitis and can be used to rule it out. - Pediatric patients: The Alvarado score and Pediatric Appendicitis Score (PAS) are useful in excluding acute appendicitis. The AIR score has shown the highest discriminating power in children. Imaging Studies: - A combination of ultrasound (US) and clinical scores (e.g., AIR, AAS) may improve diagnostic sensitivity and specificity and potentially reduce the need for CT scans in adults. - Point-of-care ultrasound (POCUS) is a reliable initial investigation.

Supplementary Table 11 – continued from previous page

Pathology name	Content
Appendicitis	- US findings suggestive of appendicitis include: thickened appendiceal wall, non-compressibility, diameter $> 6mm$, absence of gas in the lumen, appendicolith, hyperechoic periappendiceal fat, fluid collection (abscess), local bowel dilation and hypoperistalsis, free abdominal fluid, and lymphadenopathy. The most sensitive sign is a non-compressible appendix with a diameter $> 6mm$. - If a CT scan is required, contrast-enhanced low-dose CT is recommended. The overall sensitivity of CT for diagnosing acute appendicitis is 0.95, and specificity is 0.94. - Pregnant patients: For suspected appendicitis, graded compression transabdominal US is the preferred initial imaging method. If US is inconclusive, MRI is recommended if available. MRI sensitivity is 90.5%-94%, and specificity is 97%-98.6%. - Pediatric patients: US is the first-line imaging study. If US is inconclusive, the choice of second-line imaging (e.g., repeat US, CT, MRI) depends on local availability and expertise. MRI can differentiate perforated from non-perforated AA with high specificity.
Cholecystitis	Diagnostic Basis: - Diagnosis relies on a combination of detailed history, complete physical examination, laboratory tests, and imaging investigations; no single feature is sufficient to confirm or exclude the diagnosis. - History and Clinical Examination: - Fever, right upper quadrant pain or tenderness, vomiting, or intolerance to fatty foods. - Positive Murphy's sign. Laboratory Tests: - Elevated C-reactive protein, elevated white blood cell count. Imaging Studies: - Imaging shows signs suggestive of gallbladder inflammation. - Abdominal ultrasound is the preferred initial imaging technique; its overall sensitivity for diagnosing acute cholecystitis is 81%, and specificity is 83%.

Supplementary Table 11 – continued from previous page

Pathology name	Content
Cholecystitis	- Compared to other imaging methods, hepatobiliary iminodiacetic acid (HIDA) scan has the highest sensitivity and specificity for the diagnosis of acute cholecystitis (sensitivity 84.2%-89.3%, specificity 66.8%-79%). - CT has poor diagnostic accuracy for acute cholecystitis (sensitivity 59.8%). - MRI is as accurate as abdominal ultrasound.
Diverticulitis	Clinical Severity: - Diverticulitis varies in severity, from uncomplicated phlegmonous diverticulitis to complicated diverticulitis with abscess and/or perforation. Imaging Studies (CT is crucial for diagnosis and staging): - CT imaging is the primary tool for diagnosing and staging ALCD. - Neff CT Staging (Diagnostic Features): - Stage 0 (Uncomplicated): diverticula, wall thickening, increased density of pericolic fat. - Stage 1: Locally complicated with local abscess. - Stage 2: Complicated with pelvic abscess. - Stage 3: Complicated with distant abscess. - Stage 4: Complicated with other distant complications (e.g., pneumoperitoneum with abundant free fluid). Ambrosetti CT Classification (Diagnostic Features): - Moderate diverticulitis: Localized sigmoid wall thickening ($\geq 5mm$) and pericolic fat stranding. - Severe diverticulitis: Wall thickening accompanied by abscess, or extraluminal gas, or extraluminal contrast. Kaiser Modified Hinchey Classification (CT Findings): - Stage 0: Mild clinical diverticulitis. - Stage Ia: Confined pericolic inflammation. - Stage Ib: Confined pericolic abscess. - Stage 2: Pelvic or distant intra-abdominal abscess. - Stage 3: Generalized purulent peritonitis. - Stage 4: Fecal peritonitis at presentation. Mora Lopez Modified Neff Staging (CT Findings):

Supplementary Table 11 – continued from previous page

Pathology name	Content
	- Stage Ia: Localized pneumoperitoneum (in the form of gas bubbles). - Stage Ib: Abscess $< 4cm$.
Pancreatitis	Diagnostic Criteria (at least two of the following three): - Abdominal pain consistent with the disease. - Biochemical evidence of pancreatitis (serum amylase and/or lipase greater than three times the upper limit of normal). The diagnostic cutoff for serum amylase and lipase is normally defined as three times the upper limit of normal. - Characteristic findings from abdominal imaging. Laboratory Tests: - Serum lipase is considered a more reliable diagnostic marker of AP than serum amylase. (Amylase sensitivity and specificity are 72% and 93%, respectively; lipase 79% and 89%, respectively). - Trypsinogen-2 dipstick test for AP has a sensitivity of 82% and specificity of 94%. Imaging Studies: - Ultrasound should be performed on admission to determine the etiology of acute pancreatitis (e.g., biliary). - When the diagnosis is uncertain, CT provides good evidence of the presence or absence of pancreatitis, especially to rule out secondary perforation peritonitis or mesenteric ischemia. - All patients with severe acute pancreatitis need assessment with contrast-enhanced CT (CE-CT) or MRI (optimal timing for the first CE-CT assessment is 72-96 hours after symptom onset). CE-CT can detect peripancreatic necrosis after 72 hours from onset. - The CT Severity Index (Balthazar score) grades pancreatitis based on the degree of inflammation, presence of fluid collections, and extent of necrosis (Grade A: Normal pancreas; B: Pancreatic enlargement; C: Pancreatic inflammation and/or peripancreatic fat; D: Single peripancreatic fluid collection; E: ≥ 2 fluid collections and/or retroperitoneal air. Necrosis score is based on the percentage of non-enhancement of the gland).

Supplementary Table 11 – continued from previous page

Pathology name	Content
Pericarditis	Diagnostic Criteria: - Pericarditic chest pain: Typically sharp and pleuritic, improved by sitting up and leaning forward. - Pericardial friction rub: A superficial scratchy or squeaking sound best heard with the diaphragm of the stethoscope over the left sternal border. - New widespread ST-elevation or PR depression on ECG. - Pericardial effusion (new or worsening). Blood Tests: - Elevation of markers of inflammation (i.e., C-reactive protein, erythrocyte sedimentation rate, and white blood cell count). - Elevation of markers of myocardial injury (i.e., creatine kinase, troponin), especially when myocarditis is present. Imaging Studies: - Electrocardiogram (ECG): New widespread ST-segment elevation or PR depression may be seen in the acute phase. - Chest X-ray: Generally normal; an increased cardiothoracic ratio only occurs with pericardial effusions exceeding 300 mL. Signs of pleuropericardial involvement may be found. - Echocardiography: Recommended in all patients with suspected acute pericarditis; it is the first-line imaging test to detect pericardial effusion and its amount, and to assess its hemodynamic impact. - CT and Cardiac Magnetic Resonance (CMR): Can provide evidence of pericardial thickening, effusion, calcification, and pericardial inflammation (e.g., late gadolinium enhancement on CMR). Other: - Systemic signs of infection or inflammation such as fever and leukocytosis may be present.
Pneumonia	Physical Examination: - Fever, tachypnea, etc. Blood Tests: - Abnormal white blood cell count (elevated, or decreased in severe infection).

Supplementary Table 11 – continued from previous page

Pathology name	Content
Pneumonia	- Elevated inflammatory markers (e.g., C-reactive protein, procalcitonin), but procalcitonin is not recommended to determine the need for initial antibacterial therapy. Imaging Studies: - Chest X-ray or CT: Confirms the presence of pulmonary infiltrates. (Multilobar infiltrates are a CAP severity criterion). Microbiological Tests (for etiological diagnosis, not for diagnosing pneumonia itself): - Gram stain and culture of lower respiratory secretions (e.g., sputum, endotracheal aspirates). - Blood cultures (recommended in specific situations, e.g., severe CAP, or if empirically treating for MRSA or P. aeruginosa). - Urinary antigen testing (for S. pneumoniae and Legionella spp., recommended in specific situations, e.g., severe CAP, or if epidemiological factors suggest Legionella). - Testing respiratory samples for influenza virus (rapid influenza molecular assay is preferred over rapid influenza diagnostic antigen test). Other: - Respiratory symptoms such as cough, sputum production, and pleuritic chest pain may be present - Confusion, hypoxemia (PaO_2/FiO_2 $ratio < 250\%$ is a CAP severity criterion) may be present.
Pulmonary Embolism	Clinical Features (Non-specific): - Symptoms: Common symptoms include acute-onset dyspnoea, pleuritic chest pain, and cough. Others may include haemoptysis, pre-syncope or syncope, and unilateral leg swelling and pain (suggestive of deep vein thrombosis). - Signs: Common signs include tachypnoea (respiratory rate ¿20 breaths/min) and tachycardia (heart rate $>$ 100 bpm). Others may include signs of deep vein thrombosis (e.g., limb oedema, tenderness) and fever (usually $< 39°C$). The diagnostic process usually combines clinical probability assessment with ancillary tests.

Supplementary Table 11 – continued from previous page

Pathology name	Content
Pulmonary Embolism	Blood Tests: - D-dimer: In patients with low or intermediate clinical probability, a negative D-dimer test helps to exclude pulmonary embolism. It has high sensitivity but low specificity. Imaging Studies: - Computed Tomography Pulmonary Angiography (CTPA): The principal imaging test for the diagnosis of PE, directly showing thrombi. - Lung Scintigraphy (V/Q scan): An alternative imaging test when CTPA is unavailable or contraindicated. A normal V/Q scan excludes PE; a high-probability scan confirms PE. - Lower Limb Compression Ultrasonography (CUS): Used to detect DVT. In a patient with suspected PE, the detection of DVT by CUS usually confirms venous thromboembolism, and treatment is initiated accordingly. - Echocardiography: Not a primary diagnostic test for suspected PE. For patients with suspected high-risk PE (with haemodynamic instability), bedside echocardiography showing signs of right ventricular (RV) overload or dysfunction (e.g., RV dilatation, RV free wall hypokinesis, paradoxical septal motion, dilated pulmonary artery, increased tricuspid regurgitation velocity) can support clinical decision-making if CTPA is not immediately available. For non-high-risk patients, it is mainly used for risk stratification. Electrocardiogram (ECG): - The ECG in PE patients is often abnormal but lacks specificity. Possible signs include tachycardia, $S_1Q_3T_3$ pattern, incomplete or complete right bundle branch block, T-wave inversion in precordial leads ($V_1 - V_4$), and P pulmonale, among other signs of RV strain.

S10 Architectures of MACD framework and MACD-human Collaboration Workflow

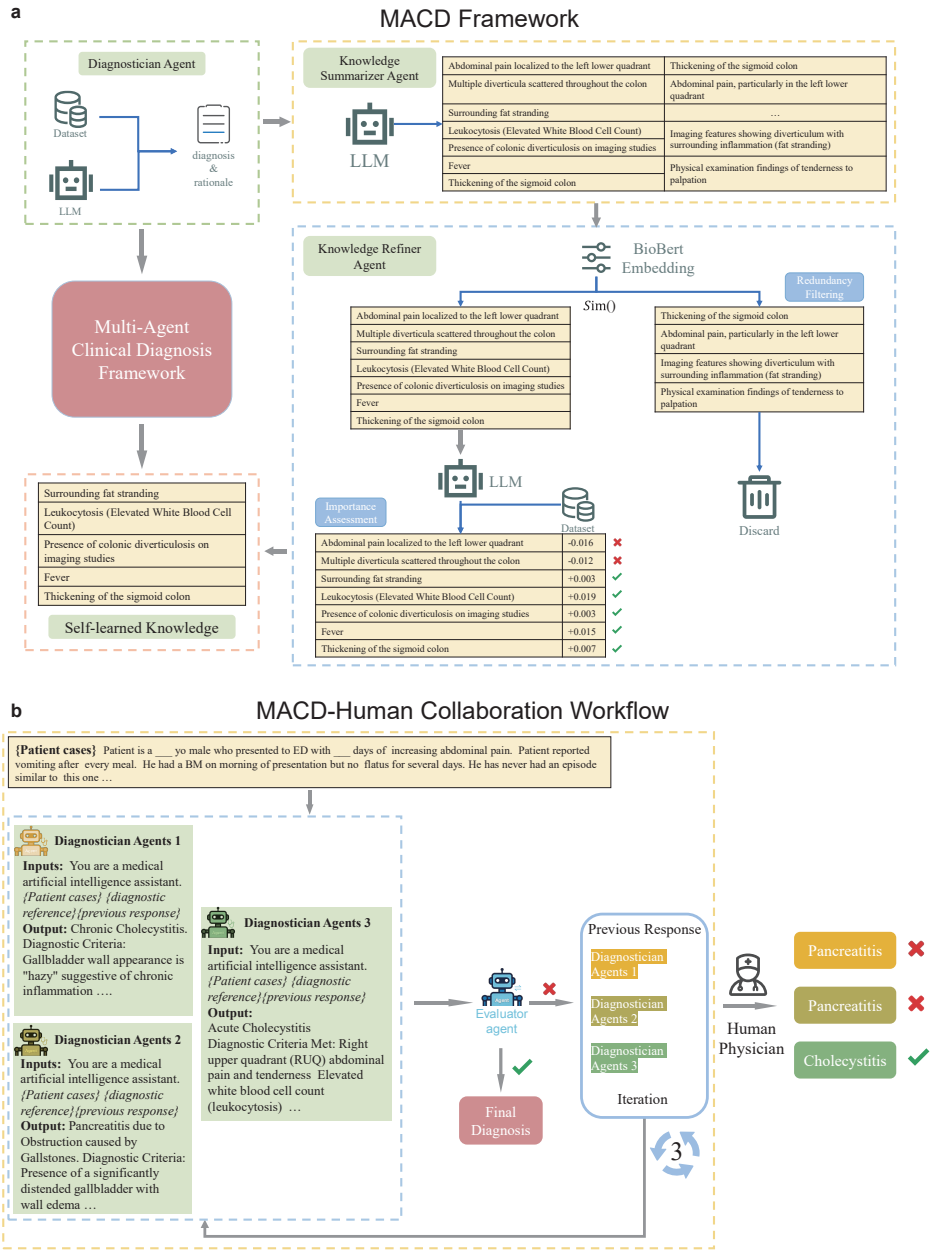

Supplementary Figure 2: **Architectures of MACD framework and MACD-human collaboration workflow.** (a) The multi-agent clinical diagnosis framework that is composed of diagnostician agents, knowledge summarizer agent and knowledge refiner agent. (b) The MACD-human collaboration workflow that is composed of three diagnostician agents, one evaluator agent and human physicians.

S11 Prompt Template of the Diagnostician Agent

{system_tag_start} You are a medical artificial intelligence assistant. You directly diagnose patients based on the provided information to assist a doctor in his clinical duties. Your goal is to correctly diagnose the patient. Based on the provided information you will provide the diagnostic criteria of the most confident pathology. Don't write any further information. Provide a single diagnosis along with the most relevant diagnostic criteria.{system_tag_end} {user_tag_start} Provide the most relevant diagnostic criteria of the following patient with no more other information. {diagnostic_guidelines} {diagnostic_reference} {input} {user_tag_end} {ai_tag_start} Final Diagnosis and diagnostic criteria:

S12 Prompt Template of the Knowledge Summarizer Agent

[Role]
You are a medical artificial intelligence assistant. Your task is to review the given report and summarize the diagnostic evidence for the identified disease.
[/Role]

[INSTRUCTIONS]
1. Analyze the report and identify the main disease.
2. Summarize the diagnostic evidence into two structured categories:
- General Criteria: The 5 most relevant common clinical manifestations and diagnostic findings typically associated with the disease.
- Rare Criteria: The 5 most relevant specific or unique clinical manifestations and diagnostic findings observed in a subset of patients with the disease.
3. Only one response is required. Do not repeat or provide multiple outputs.
4. Ensure the summarized content is specific, concise, and directly extracted from the input report. Avoid adding explanations, references, or unnecessary details.
5. Strictly adhere to the specified output format.
[/INSTRUCTIONS]

[REPORT]
{correct_diag_result}
[/REPORT]

[OUTPUT FORMAT]

Disease: (Identified disease)

General Criteria:

1. (Most relevant common clinical manifestation or diagnostic finding)
2. (Most relevant common clinical manifestation or diagnostic finding)
3. (Most relevant common clinical manifestation or diagnostic finding)
4. (Most relevant common clinical manifestation or diagnostic finding)
5. (Most relevant common clinical manifestation or diagnostic finding)

Rare Criteria:

1. (Most relevant specific or unique clinical manifestation or diagnostic finding)
2. (Most relevant specific or unique clinical manifestation or diagnostic finding)
3. (Most relevant specific or unique clinical manifestation or diagnostic finding)
4. (Most relevant specific or unique clinical manifestation or diagnostic finding)
5. (Most relevant specific or unique clinical manifestation or diagnostic finding)

[/OUTPUT FORMAT]

[REQUIEMENTS]

- Each category must contain exactly 5 summarized criteria. If fewer than 5 rare criteria are available, stat "Not available" for the remaining items.
- Focus solely on diagnostic evidence relevant to clinical practice, directly extracted from the report.
- Ensure the response is generated only once, with no repetitions or additional outputs.

Your response must strictly adhere to the above format. Any repeated or additional outputs will be considered a deviation.

[/REQUIEMENTS]

[OUTPUT]

S13 Comparative Analysis of Semantic Similarity Differences

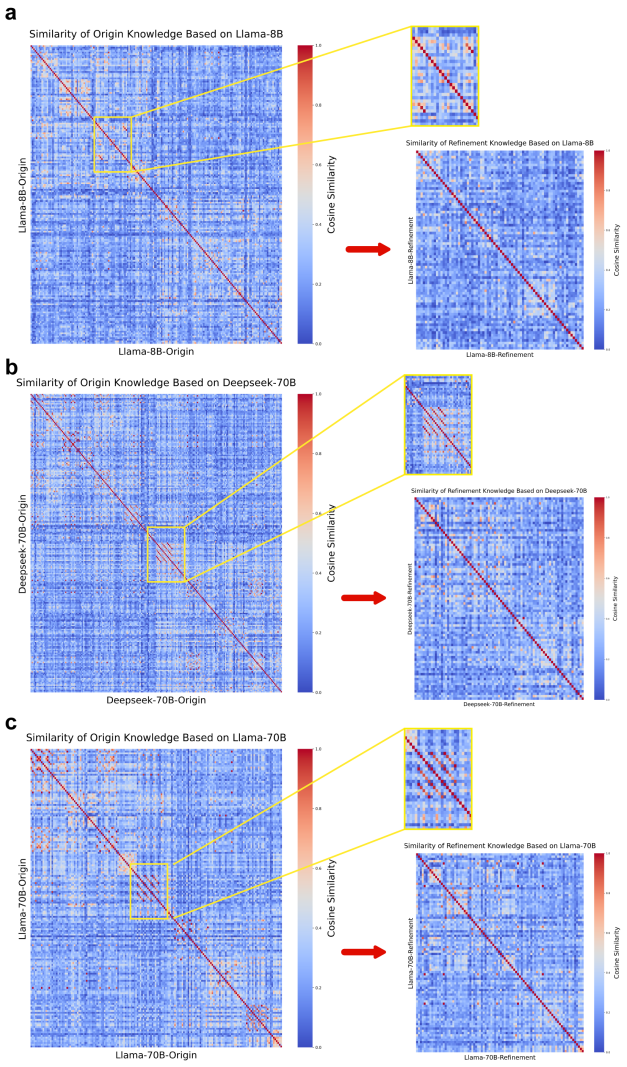

Supplementary Figure 3: **Differences in semantic similarity of Self-Learned Knowledge through knowledge refiner agent.** (a) Differences of the Self-Learned Knowledge of Llama-8B model. (b) Differences of the Self-Learned Knowledge of the DeepSeek-70B model. (c) Differences of the Self- of the Llama-70B model.

S14 Prompt Template of the MACD-human Collaboration Workflow

{system_tag_start}You are a senior medical artificial intelligence assistant. Your primary duty is to assist a doctor by verifying previous diagnostic opinions and forming an independent diagnosis based on the patient's complete situation. Based on the provided information you will provide the diagnostic criteria of the most confident pathology. Don't write any further information. Provide a single diagnosis along with the most relevant diagnostic criteria.{system_tag_end}{user_tag_start}Provide the most relevant diagnostic criteria of the following patient with no more other information.{diagnostic_reference}{input}

The provided diagnostic results are for reference only. Given that prior opinions may be inconsistent, you must conduct an impartial evaluation and not simply echo others' findings. @@@ Past Diagnosis Results @@@ {past_diagnosis_results}

{user_tag_end}{ai_tag_start}Final Diagnosis and diagnostic criteria:

S15 Diagnosis Definitions

Target Disease	Location	Modifiers
pneumonia	lung	infect
		pneumonitis
	pneumonia	acute
		pneumonitis
	respiratory	infection
Pulmonary embolism	pulmonary	embolism
		embolus
		thrombus
pericarditis	pericard	inflammatory disease
	pericardial	pericardial inflammation
	pericard	effusion
	pericardial	effusion
		thickening

S16 Conceptual Reliability Evaluation Metric for Self-Learned Knowledge

Supplementary Table 12: Conceptual Relevance Evaluation Metric for Self-Learned Knowledge

Criteria	**Score**
This concept is directly and closely related to the target disease	5
The concept is significantly related to the target disease	4
There is a certain correlation between the concept and the target disease	3
The connection between the concept and the target disease is relatively indirect and weak	2
This concept is not substantially related to the target disease	1

S17 Evaluation Results of the Concept Reliability by Human Experts

Supplementary Table 13: Evaluation Results of the Concept Relevance by Human Experts

Model	pathology						
	Appendicitis	Cholecystitis	Diverticulitis	Pancreatitis	Pericarditis	Pneumonia	Pulmonary embolism
Llama -8B	3.73 ± 0.16	3.26 ± 0.51	3.52 ± 0.58	3.75 ± 0.22	2.92 ± 0.66	3.62 ± 0.54	3.10 ± 0.35
DeepSeek -70B	3.95 ± 0.16	$\mathbf{3.89} \pm 0.26$	3.81 ± 0.34	$\mathbf{4.17} \pm 0.09$	$\mathbf{3.74} \pm 0.52$	3.72 ± 0.57	3.62 ± 0.51
Llama -70B	$\mathbf{4.21} \pm 0.15$	3.77 ± 0.21	$\mathbf{4.03} \pm 0.42$	$\mathbf{4.17} \pm 0.34$	3.28 ± 0.33	$\mathbf{4.00} \pm 0.47$	$\mathbf{4.08} \pm 0.43$

S18 Physicians Evaluation Website

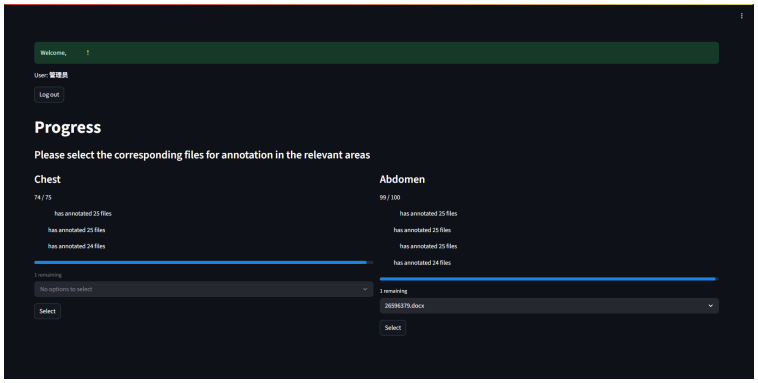

Supplementary Figure 4: Case selection page of evaluation website.

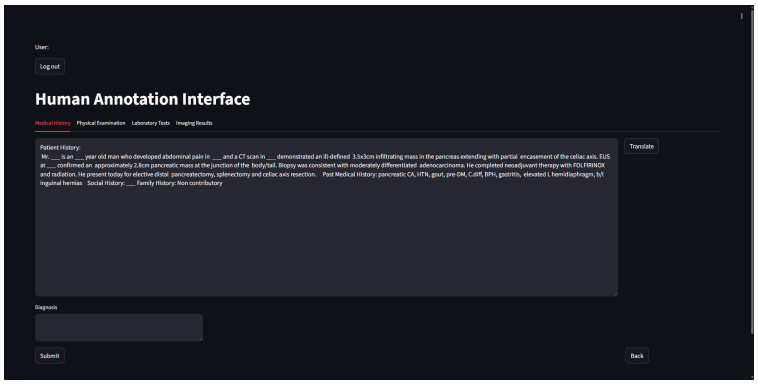

Supplementary Figure 5: Diagnosis page of evaluation website for physicians.

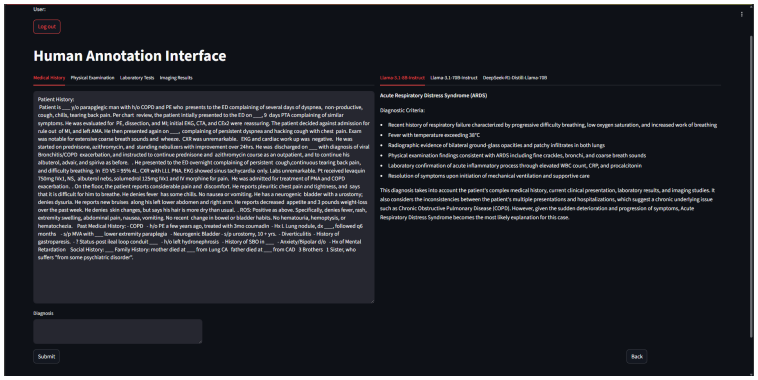

Supplementary Figure 6: Diagnosis page of evaluation website for MACD-huamn collaboration workflow.